PHYSICAL REVIEW E VOLUME 55, NUMBER 2 FEBRUARY 1997

Bead-Fourier path-integral Monte Carlo method applied to systems of identical particles

P. N. Vorontsov-Velyaminov, M. O. Nesvit, and R. I. Gorbunov
Faculty of Physics, St. Petersburg State University, 198904, St. Petersburg, Russia

(Received 2 July 1996)

To make the path-integral Monte Carlo (PIMC) method more effective and practical in application to systems of identical particles with strong interactions, we introduce a combined bead-Fourier (BF) PIMC approach with the ordinary bead method and the Fourier PIMC method of Doll and Freeman [J. Chem. Phys. **80**, 2239 (1984); **80**, 5709 (1984)] being its extreme cases. Optimal choice of the number of beads and of Fourier components enables us to reproduce reliably the ground-state energy and electron density distribution in the H atom as well as the exact data for the harmonic oscillator. Applying the BF method to systems of identical particles we use the procedure of simultaneous accounting for all classes of permutations suggested in the previous work [Phys. Rev. A **48**, 4075 (1993)] with subsequent symmetrization of the exchange factor in the weight function to make the sign problem milder. A procedure of random walk in the spin space enables us to obtain spin-dependent averages. We derived exact partition functions and canonical averages for a model system of N noninteracting identical particles ($N=2,3,4,\ldots$) with the spin (fermions or bosons) in a d-dimensional harmonic field ($d=1,2,3$) that provided a reliable test of the developed MC procedures. Simulations for $N=2,3$ reproduce well the exact dependencies. Further simulations showed how gradual switching on of the electrostatic repulsion between particles in this system results in significant weakening of the exchange effects. [S1063-651X(97)07601-0]

PACS number(s): 02.70.Lq, 03.65.−w, 05.30.Fk

I. INTRODUCTION

Development of path-integral Monte Carlo (PIMC) methods for finite-temperature simulations of quantum systems of identical particles (particularly fermions) remains a challenging problem of statistical mechanics [1–6].

In a previous work [2] a PIMC method was suggested to simulate equilibrium properties of an N-electron system. The main points of the approach were (1) the sum over permutations was reduced to the sum over classes; (2) expressions for distribution functions over absolute values of the total spin and its projection were constructed, enabling calculations of spin-dependent averages; (3) the partition function was presented in a form in which contributions from all classes of permutations are accounted for in the weight function simultaneously, and hence there is no need to make MC transitions between different permutations in the course of a random walk in the coordinate space.

It should also be noted that continuous trajectories representing each quantum particle in the PIMC method were approximated in [2] by a finite number of vertices (‘‘beads’’); this approximation usually being called the ‘‘bead method’’ (e.g., [7,8]). Meanwhile there exists another means of presenting continuous trajectories of quantum particles, that is, the Fourier method [9,10] introduced into PIMC simulations by Doll and Freeman [11] and recently applied by Chakravarty [5] to simulate systems of identical particles. In the Fourier PIMC method there is only one ‘‘bead’’ per particle and all the multitude of trajectories starting and ending at this bead is presented by a Fourier series with an infinite set of amplitudes a_k. The functional integral representing the partition function is transformed, in this case, into an integral over coordinates of this single bead and integrals over an infinite set of Fourier amplitudes. As long as the set of a_k is infinite, the expression for the partition function in the Fourier method is exact. The approximation used implies neglecting all higher harmonics with $k>k_{\max}$. Hence, for each set of input physical parameters (e.g., temperature, potential), it is necessary to choose such a value of $k_{\max}$ that its further increase does not affect the output MC averages. The Fourier PIMC method was successfully used in several recent works [7,8,12] and proved to be superior in some aspects to the bead method (e.g., [8]). It should be pointed out, however, that the number of harmonics used in calculations even for systems of heavy particles with relatively weak interactions and with no accounting for exchange attains several hundred [12]. This means, in particular, that the number of integration points in the potential part of the action should be also several hundred. In the case of electrons in strong external fields of nuclei, if the Fourier method is used, a further increase of $k_{\max}$ seems to be necessary, and that can make such calculations impractical. On the other hand, our previous computational experience in the framework of the bead method has shown that for systems with strong interactions (e.g., an electron in a hydrogen atom) we encounter rather slow convergence of results when the number of beads is increased with some other undesirable effects. In order to make PIMC calculations practical and more reliable in conditions of strong interactions, we develop a general (combined) method which unifies two existing approaches and includes them as its extreme cases. While in the bead method the number of variables is Nnd, N and d being the number of particles and dimensionality and n the number of beads, in the Fourier method we have $Nd(1+k_{\max})$ variables. In the bead-Fourier variant of the PIMC method it becomes $Nnd(1+k_{\max})$ (see Sec. II). Although the latter exceeds both of the former it appears possible to choose an optimal computational regime with relatively small values of $k_{\max}$ (about 3–6) and simultaneously an optimal number of beads in order to provide convergence and good accuracy of results at modest computation expense. It would also be clear from our test calculations that the extreme regimes (pure bead or pure Fourier procedures) are not the optimal ones.

Formulation of the suggested bead-Fourier PIMC method for systems of distinguishable and identical particles is presented in Sec. II. In this section we also construct the partition function in a form symmetrical with respect to permutations. This makes contributions of all beads to exchange equal and thus lowers computational errors. Finally still another form of the partition function is obtained, enabling us to formulate a MC procedure with additional random walk in the space of total spin or its projection. This provides a straightforward means to calculate spin-dependent averages. In Sec. III we obtain the bead-Fourier forms for kinetic and potential energy estimators in $k_{\max}$ approximation. For kinetic energy both ‘‘primitive’’ and virial forms are obtained. In order to test computer algorithms created according to schemes adopted in Secs. II and III, it is desirable to reproduce existing exact results for model systems. Exact expressions for the partition function, internal energy, and the average of the square of total spin for a system of N noninteracting identical particles in a d-dimensional external harmonic field, are obtained in Sec. IV. In Sec. V we describe main features of algorithms and programming. The results illustrating feasibility of the suggested method are presented in Sec. VI. Final remarks and conclusions are made in Sec. VII. Some relevant analytical calculations are carried out in the Appendix.

II. BEAD-FOURIER PATH-INTEGRAL MONTE CARLO METHOD

A. A single particle in one dimension

We start with a single quantum particle of mass m in one-dimensional external potential $V(x)$ at inverse temperature β. The relevant partition function can be expressed as a functional integral [9,13]

$$Z=\mathrm{Tr}\,\rho=\oint D(x(u))\exp[-S(x(u))], \tag{1}$$

where $\oint D(x(u))$ denotes integration over all closed trajectories $x(u)$ $(x(0)=x(\beta\hbar))$, and $S(x(u)) =1/\hbar\int_0^{\beta\hbar}\{[m\dot{x}(u)^2/2]+V(x(u))\}du$—action on Euclidean time u. Equation (1) can also be expressed as

$$Z=\int dx\int_{x(0)=x}^{x(\beta\hbar)=x}D(x(u))\exp[-S(x(u))], \tag{2}$$

with the external one-dimensional ordinary integration, and the internal functional integral over all closed trajectories with the initial and final points at fixed x. This expression was the basis for the Fourier PIMC method of Doll and Freeman [11]. To create the combined method we take the next step: we divide the whole ‘‘time’’ interval $[0,\beta\hbar]$ into n parts (we shall consider them equal, though it is not necessary) and introduce the following notations: $u_1=0$, $u_2=[\beta\hbar/n],\dots,$ $u_j=[(j-1)\beta\hbar/n],\dots,$ $u_n=[(n-1)\beta\hbar/n]$, $u_{n+1}=\beta\hbar$; $\Delta u=[\beta\hbar/n]\equiv\varepsilon$. Let also $x(u_1)=x_1$, $x(u_2)=x_2,\dots,$ $x(u_j)=x_j,\dots,$ $x(u_n)=x_n$, $x(u_{n+1})=x_1$. Then the partition function Z can be expressed as follows:

$$Z=\int dx_1\dots x_n\int_{x_1}^{x_2}D(x(u))\int_{x_2}^{x_3}D(x(u))\dots\int_{x_n}^{x_1}D(x(u))$$
$$\times\exp\left\{-\frac{1}{\hbar}\sum_{j=1}^{n}\int_{u_j}^{u_{j+1}}\left[\frac{m\dot{x}(u)^2}{2}+V(x(u))\right]du\right\}, \tag{3}$$

where $\int dx_1\dots x_n$ are ordinary one-dimensional integrals, and $\int_{x_j}^{x_{j+1}}D(x(u))$ are functional integrals over trajectories starting at x_j and ending at x_{j+1}. Now introducing a designation

$$S_j(x(u))=\frac{1}{\hbar}\int_{u_j}^{u_{j+1}}\left[\frac{m\dot{x}(u)^2}{2}+V(x(u))\right]du,$$

we can rewrite Eq. (3) as

$$Z=\int\prod_{1\leqslant j\leqslant n}\left(dx_j\int_{x_j}^{x_{j+1}}D(x(u))\exp[-S_j(x(u))]\right) \tag{4}$$

with the condition $x_{n+1}=x_1$.

Following [10] for each interval x_j,x_{j+1} we consider: $x_j(u)=x_{cj}(u)+y_j(u)$, where $x_{cj}(u)=x_j+(x_{j+1}-x_j)(u-u_j)/(u_{j+1}-u_j)$ is a linear function, $x_{cj}(u_j)=x_j$, $x_{cj}(u_{j+1})=x_{j+1}$, and $y_j(u_j)=y_j(u_{j+1})=0$. So the component $y_j(u)$ for each interval can be presented as a Fourier sine expansion

$$y_j(u)=\sum_{1\leqslant k<\infty}a_{jk}\sin\frac{k\pi(u-u_j)}{u_{j+1}-u_j}.$$

The kinetic energy term in the action $S_j(x(u))$, can be expressed explicitly. Using the designation $\varepsilon\equiv u_{j+1}-u_j$, we get the derivative $\dot{x}$

$$\dot{x}=\frac{(x_{j+1}-x_j)}{\varepsilon}+\sum_k a_{jk}\left[\frac{k\pi}{\varepsilon}\right]\cos\frac{k\pi(u-u_j)}{\varepsilon}. \tag{5}$$

Introduce a new variable $\xi=(u-u_j)/\varepsilon$, so that $u=u_j\rightarrow\xi=0$, $u=u_{j+1}\rightarrow\xi=1$, $du=\varepsilon d\xi$, and $\int_{u_j}^{u_{j+1}}du$ transforms into $\varepsilon\int_0^1 d\xi$. For $\dot{x}^2$ we now obtain

$$\dot{x}(u)^2=\frac{(x_{j+1}-x_j)^2}{\varepsilon^2}+2\,\frac{x_{j+1}-x_j}{\varepsilon}\sum_k a_{jk}\left[\frac{k\pi}{\varepsilon}\right]\cos k\pi\xi$$
$$+\left(\sum_k a_{jk}\left[\frac{k\pi}{\varepsilon}\right]\cos k\pi\xi\right)^2. \tag{6}$$

As long as $\int_0^1\cos k\pi\xi\,d\xi=0$ for $k=1,2,\dots$ the kinetic part of the action on the jth interval in Eq. (4) is

$$\frac{1}{\hbar}\int_{u_j}^{u_{j+1}}\frac{m\dot{x}^2}{2}\,du=\frac{m\varepsilon}{2\hbar}\int_0^1\dot{x}(\xi)^2d\xi$$

$$=\frac{m}{2\hbar}\left[\frac{(x_{j+1}-x_j)^2}{\varepsilon}+\sum_k\,(k\pi)^2\,\frac{a_{jk}^2}{2\varepsilon}\right]$$

$$=(\widetilde{x}_{j+1}-\widetilde{x}_j)^2+\sum_k\,\frac{(k\pi)^2}{2}\,\widetilde{a}\,{}_{jk}^2. \tag{7}$$

In the latter expression we introduced dimensionless coordinates and Fourier amplitudes: $\widetilde{x}\equiv x/\text{unit}$, $\widetilde{a}\equiv a/\text{unit}$; where unit $\equiv\sqrt{\Lambda_n^2/\pi}$; $\Lambda\,{}_n^2=(\Lambda^2/n)$; $\Lambda\equiv\sqrt{(\beta h^2)/(2\pi m)}$, and Λ is the thermal de Broglie wavelength.

The potential part of the action now can be written in new variables and units as

$$\frac{1}{\hbar}\int_{u_j}^{u_{j+1}}V(x(u))du=\frac{\beta}{n}\int_0^1V[x_j(\xi)]d\xi\equiv\int_0^1\widetilde{V}[\widetilde{x}_j(\xi)]d\xi, \tag{8}$$

where $\widetilde{V}(\widetilde{x})=(\beta/n)V(\text{unit}\cdot\widetilde{x})$; $\widetilde{x}_j(\xi)=\widetilde{x}_j+(\widetilde{x}_{j+1}-\widetilde{x}_j)\xi+\Sigma_k\widetilde{a}_{jk}\sin k\pi\xi$. As a result the action S_j is

$$S_j(\{\widetilde{a}_{jk}\})=(\widetilde{x}_{j+1}-\widetilde{x}_j)^2+\sum_k\,\frac{(k\pi)^2}{2}\,\widetilde{a}\,{}_{jk}^2+\int_0^1\widetilde{V}[\widetilde{x}_j(\xi)]d\xi. \tag{9}$$

Now again following [10] we can pass from the functional integral over trajectories $\int_{x_j}^{x_{j+1}}D(x(u))$ to the integral over Fourier coefficients a_{jk}

$$\int_{x_j}^{x_{j+1}}D(x(u))\exp[-S_j(x(u))]=\int J_j\prod_k\,d\widetilde{a}_{jk}$$
$$\times\exp[-S_j(\{\widetilde{a}_{jk}\})]. \tag{10}$$

Here $J_j=(1/\Lambda_n)\Pi_k[(\pi k/\sqrt{2})(1/\Lambda_n)]$ is the Jacobian of the transformation. As a result the partition function (4) becomes

$$Z=\int d\widetilde{\tau}e^{-H},$$

$$H=\sum_{1\leqslant j\leqslant n}\left[(\widetilde{x}_{j+1}-\widetilde{x}_j)^2+\sum_k\,\frac{(k\pi)^2}{2}\,\widetilde{a}\,{}_{jk}^2+\int_0^1\widetilde{V}[\widetilde{x}_j(\xi)]d\xi\right] \tag{11}$$

and

$$d\widetilde{\tau}=\prod_{1\leqslant j\leqslant n}\left(\frac{d\widetilde{x}_j}{\sqrt{\pi}}\prod_{k=1}^{\infty}\,\frac{\pi k}{\sqrt{2\pi}}\,d\widetilde{a}_{jk}\right).$$

H is an effective Hamiltonian.

B. N distinguishable particles in three dimensions

The bead-Fourier form of the partition function for a three-dimensional system of N distinguishable particles can be obtained in a way similar to the previous result, Eq. (11). Starting with the procedure described in Sec. II A we obtain 3N-dimensional analogies of Eqs. (3) and (4). Further transformations yield Z in the final form

$$Z_D=\int d\widetilde{\tau}e^{-H},$$

$$H=\sum_{1\leqslant j\leqslant n}\left[(\widetilde{q}_{j+1}-\widetilde{q}_j)^2+\sum_k\,\frac{(k\pi)^2}{2}\,\widetilde{A}\,{}_{jk}^2+\int_0^1\widetilde{V}[\widetilde{q}_j(\xi)]d\xi,\right. \tag{12}$$

with the condition $\widetilde{q}_{n+1}=\widetilde{q}_1$. The designations in Eq. (12) are

$$\widetilde{q}_j=(\ldots,\vec{r}_{ij},\ldots),\quad \vec{r}_{ij}=(\widetilde{x}_{i1j},\widetilde{x}_{i2j},\widetilde{x}_{i3j}),$$

and

$$\widetilde{A}_{jk}=(\ldots,\widetilde{a}_{isjk},\ldots)\quad\text{at }\; i=1,\ldots,N;\;\; s=1,2,3.$$

So that

$$\widetilde{q}_j(\xi)=[\ldots,\widetilde{x}_{isj}(\xi),\ldots];$$

$$\widetilde{x}_{isj}(\xi)=\widetilde{x}_{isj}(1-\xi)+\widetilde{x}_{is(j+1)}\xi+\Sigma_k\widetilde{a}_{isjk}\sin k\pi\xi.$$

And

$$d\widetilde{\tau}=\prod_{\substack{1\leqslant j\leqslant n\\1\leqslant i\leqslant N\\s=1,2,3}}\left[\frac{1}{\sqrt{\pi}}\,d\widetilde{x}_{isj}\prod_k\,\frac{k\pi}{\sqrt{2\pi}}\,d\widetilde{a}_{isjk}\right].$$

Both Eqs. (11) and (12) are exact expressions for any finite number of beads n as long as the set of k is infinite. In both expressions the exp factor can be treated as an ‘‘effective Hamiltonian’’ of some ‘‘classical’’ system. It is also evident that expressions (11) and (12) include the ‘‘pure Fourier’’ method of Doll and Freeman [11] and the ‘‘pure bead’’ method as the extreme cases. In the case $n=1\Pi_{1\leqslant j\leqslant n}dx_j\rightarrow dx$, $\Sigma_{1\leqslant j\leqslant n}(x_{j+1}-x_j)^2$ disappears in Eq. (11) [in Eq. (12) analogous changes occur], and we come to the partition function Z in pure Fourier form [11]. On the other hand, if we remove $\Pi_kd\widetilde{a}_k$ and Σ_k in Eqs. (11) and (12), i.e., put $k_{\max}=0$ we come to the vertex (bead) method. In the latter case the only difference is that in a pure bead method the potential centers are located on beads, whereas in our extreme case the potential is uniformly spread along the straight lines between beads. This allows us to get a better estimation for the potential energy than in a pure bead method.

C. N identical particles in three dimensions

Now we consider a system of N indistinguishable particles (fermions or bosons) in three-dimensional space. Expressing the density matrix $\rho^{(A,S)}$ as an antisymmetric (symmetric) sum of density matrices for a system of N distinguishable particles $\rho^{(D)}$ we get the following expression for the partition function [13]:

$$
\begin{aligned}
Z&=\mathrm{Tr}(\rho^{(A,S)})\\
&=\frac{1}{N!}\sum_{\{P\}}\xi^{[P]}\int dx_1\ldots dx_N\rho^{(D)}(x_1\ldots x_N;P(x_1)\ldots P(x_N)).
\end{aligned}
\tag{13}
$$

Here x_i is a set of space coordinates and spin variables: $x_i=(\vec{r},\sigma)$, and $\int dx=\Sigma_\sigma\int d\vec{r}$, ξ equals to -1 for fermions and 1 for bosons, and $[P]$—parity of the permutation P. Below we shall consider mostly fermions ($\sigma=\pm 1/2$). The density matrix $\rho^{(D)}$ in Eq. (13) for the spin-independent Hamiltonian can be presented as $\rho^{(D)}=\rho_0^{(D)}(\vec{r}_1,\ldots,\vec{r}_N,P(\vec{r}_1),\ldots,P(\vec{r}_N))\rho_{sp}(P)$, where $\rho_0^{(D)}$ is its coordinate contribution and $\rho_{sp}(P)$ is its spin part for permutation P

$$
\rho_{sp}(P)=\delta(\sigma_1,P(\sigma_1))\ldots\delta(\sigma_N,P(\sigma_N)).
\tag{14}
$$

Substituting Eq. (14) into Eq. (13) we obtain, for the partition function Z,

$$
Z=\frac{1}{N!}\sum_{\{P\}}\xi^{[P]}K(P)Z_D(P).
\tag{15}
$$

Here $K(P)=\Sigma_{\sigma_1\ldots\sigma_N=\pm 1/2}\delta(\sigma_1,P(\sigma_1))\ldots\delta(\sigma_N,P(\sigma_N))$ is the spin contribution to the partition function and $Z_D(P)$ is the coordinate part of the partition function for the permutation P

$$
\begin{aligned}
Z_D(P)&=\int d\vec{r}_1\ldots d\vec{r}_N\rho_0^{(D)}[\vec{r}_1\ldots\vec{r}_N,P(\vec{r}_1)\ldots P(\vec{r}_N)]\\
&=\int dq\rho_0^{(D)}(q,P(q)).
\end{aligned}
\tag{16}
$$

In the latter form we used the designation $q=(\vec{r}_1,\ldots,\vec{r}_N)$ introduced earlier in Sec. II B.

Following [2] we rewrite the partition function Z (15) as a sum over classes of permutations $\{G\}$. Then $\xi^{[P]}\rightarrow\xi^{[G]}$, $K(P)\Rightarrow K(G)=2^{\Sigma_\nu C_\nu(G)}$, where $C_\nu(G)$ is the number of cycles of length ν in the given class G, so that $\Sigma_\nu C_\nu(G)$ is the total number of cycles in the class G; $Z_D(P)=Z_D(G)$, since the value of an integral over all coordinates depends only on the cycle structure of the permutation. This way the partition function becomes

$$
Z=\frac{1}{N!}\sum_G\xi^{[G]}K(G)n(G)Z_D(G)=\sum_G a_GZ_D(G),
\tag{17}
$$

where $n(G)$ is the number of permutations in the given class G [13,2]. In the last form we introduced a designation

$$
a_G=\xi^{[G]}K(G)\,\frac{n(G)}{N!}.
\tag{18}
$$

The bead-Fourier form of $Z_D(G)$ can be readily obtained from Eq. (12)

$$
Z_D(G)=\int d\tilde{\tau}\varepsilon^{-H_G},
\tag{19}
$$

where

$$
\begin{aligned}
H_G=\sum_{1\leqslant j\leqslant n}^{(G)}\Bigg[&(\tilde{q}_{j+1}-\tilde{q}_j)^2+\sum_k\frac{(k\pi)^2}{2}\tilde{A}_{jk}^2\\
&+\int_0^1\tilde{V}(\tilde{q}_j(\xi))d\xi.
\end{aligned}
$$

$\Sigma^{(G)}$ in Eq. (19) means the sum over beads on condition that $\tilde{q}_{n+1}=P_G(\tilde{q}_1)$, this being the only difference between Eqs. (12) and (19).

Now following [2] we change the order of the summation over classes and the integration over coordinates and Fourier coefficients in Eqs. (17)–(19) and we distinguish as a factor a sum of exponents containing $\tilde{q}_n$ and $\tilde{q}_{n+1}=P_G(\tilde{q}_1)$. We obtain the expression

$$
\begin{aligned}
Z&=\sum_G a_GZ_D(G)\\
&=\int d\tilde{\tau}\exp\Bigg\{-\sum_{1\leqslant j\leqslant n-1}\Bigg[(\tilde{q}_{j+1}-\tilde{q}_j)^2+\sum_k\frac{(k\pi)^2}{2}\tilde{A}_{jk}^2\\
&\quad+\int_0^1\tilde{V}(\tilde{q}_j(\xi))d\xi\Bigg]\Bigg\}\sum_G a_G\exp\Bigg\{-\Bigg[(\tilde{q}_n-P_G(\tilde{q}_1))^2\\
&\quad+\sum_k\frac{(k\pi)^2}{2}\tilde{A}_{nk}^2+\int_0^1\tilde{V}(\tilde{q}_n^G(\xi))\Bigg]\Bigg\}d\xi,
\end{aligned}
\tag{20}
$$

where $\tilde{q}_n^G(\xi)=\tilde{q}_n(1-\xi)+P_G(\tilde{q}_1)\xi+\Sigma_k\tilde{A}_{nk}\sin k\pi\xi$.

D. Symmetrization of *Z*

Now we subtract and add in the exponent in Eq. (20) the following term $(\tilde{q}_n-\tilde{q}_1)^2+\Sigma_k[(k\pi)^2/2]\tilde{A}_{nk}^2+\int\tilde{V}(\tilde{q}_n(\xi))d\xi$. So we get

$$
Z=\int d\tilde{\tau}e^{-H}W,
\tag{21}
$$

where H is determined by Eq. (12) and

$$
W=\sum_G a_G\varepsilon^{-\Delta H_G},
\tag{22}
$$

where

$$
\begin{aligned}
\Delta H_G&=H_G-H\\
&=(\tilde{q}_n-P_G(\tilde{q}_1))^2-(\tilde{q}_n-\tilde{q}_1)^2\\
&\quad+\int_0^1\tilde{V}(\tilde{q}_n^G(\xi))d\xi-\int_0^1\tilde{V}(\tilde{q}_n(\xi))d\xi\ .
\end{aligned}
$$

Then we multiply and divide the expression (21) by n and rewrite it as $1/n\Sigma_{l=1}^n$. After that we renumerate indices of the beads j in each next integral of the sum shifting them by unity with respect to the previous one. Both $d\tilde{\tau}$ and H, being a cyclic product and a sum, remain unchanged. Gathering all the terms in the sum under common integral $\int d\tilde{\tau}$ we take into account that e^{-H} is the common term. So finally we obtain again expression (21) with another (symmetrical) form of W

$$W=\sum_G \frac{a_G}{n} \sum_{1\leqslant j\leqslant n} e^{-\Delta H_G^{(j)}}. \tag{23}$$

Here

$$\Delta H_G^{(j)}=(\widetilde{q}_j-P_G(\widetilde{q}_{j+1}))-(\widetilde{q}_j-\widetilde{q}_{j+1})^2+\int_0^1 \widetilde{V}(\widetilde{q}\,{}_j^G(\xi))d\xi$$
$$-\int_0^1 \widetilde{V}(\widetilde{q}_j(\xi))d\xi \; .$$

Expression (21), for the partition function with Eq. (23) for W, is an exact one in which all beads, $1\leqslant j\leqslant n$, make an equal contribution to the exchange between particles.

E. Forms of Z with explicit averaging over total spin or over its projection

The coefficients a_G can be presented in one of the following forms [2]:

$$a_G=\sum_S a_{GS}\,, \quad a_{GS}=\mathrm{sgn}(G)(2S+1)\Omega(S,G)\,\frac{n(G)}{N!}, \tag{24}$$

$$a_G=\sum_m a_{Gm}\,, \quad a_{Gm}=\mathrm{sgn}(G)\omega(m,G)\,\frac{n(G)}{N!}, \tag{25}$$

where $\Omega(S,G)$ is the distribution over values of the total spin $S(0(1/2)\leqslant S\leqslant N/2)$ and $\omega(m,G)$ is the spin-projection distribution $(-N/2\leqslant m\leqslant N/2)$ for the class G [2]. So we can rewrite Eq. (21) in the following form:

$$Z=\sum_S Z_S=\sum_m Z_m\,, \tag{26}$$

where

$$Z_S=\int d\widetilde{\tau}e^{-H}W_S\,, \quad W_S=\sum_G \frac{a_{GS}}{n} \sum_{1\leqslant j\leqslant n} e^{-\Delta H_G^{(j)}} \tag{27}$$

and

$$Z_m=\int d\widetilde{\tau}e^{-H}W_m\,, \quad W_m=\sum_G \frac{a_{Gm}}{n} \sum_{1\leqslant j\leqslant n} e^{-\Delta H_G^{(j)}}. \tag{28}$$

This representation of the partition function allows us to make a random walk over the values of the total spin or its projection and calculate corresponding spin-dependent averages, e.g., $\langle S(S+1)\rangle$

$$\langle S(S+1)\rangle=\frac{1}{Z}\sum_S S(S+1)Z_S\,. \tag{29}$$

III. ENERGY ESTIMATORS IN THE BEAD-FOURIER FORM

A. The primitive estimator

The so-called primitive estimator for the internal energy can be obtained from the Gibbs-Helmholtz equation (e.g., [14])

$$E=\frac{\partial}{\partial\beta}\,(\beta F)=-\,\frac{\partial\,\ln Z(\beta)}{\partial\beta}, \tag{30}$$

where $Z(\beta)$ is the canonical partition function. In the simplest case (one particle in one dimension) we substitute Eq. (11) for Z into Eq. (30). Before differentiation the k approximation should be introduced, i.e., we must hold only first terms with $1\leqslant k\leqslant k_{\max}$ in the infinite sums and products over k. Then Eq. (30) yields

$$E=\langle\epsilon_K\rangle+\langle\epsilon_P\rangle, \tag{31}$$

where

$$\epsilon_K=\frac{n}{2}\,(1+k_{\max})\,\frac{1}{\beta}-\frac{\alpha}{\beta},$$

$$\alpha=\sum_{j=1}^{n}\left[(\widetilde{x}_{j+1}-\widetilde{x}_j)^2+\sum_{k=1}^{k_{\max}}\frac{(k\pi)^2}{2}\,\widetilde{a}_{jk}^2\right], \tag{32}$$

$$\epsilon_P=\frac{1}{n}\sum_{j=1}^{n}\int_0^1 V(x_j(\xi))d\xi=\frac{1}{\beta}\sum_{j=1}^{n}\int_0^1 \widetilde{V}(\widetilde{x}_j(\xi))d\xi. \tag{33}$$

Here, and below, ϵ_K and ϵ_P are estimators of kinetic and potential energies. Note that $\alpha+\beta\epsilon_P=H$ for H (11). $\widetilde{x}_j(\xi)$ is determined in Eq. (8) with Σ_k limited by $k_{\max}$. Averaging $\langle O\rangle$ in Eq. (31) implies

$$\langle O\rangle=Z^{-1}\int d\widetilde{\tau}Oe^{-H}, \tag{34}$$

where Z and H are determined in Eq. (11).

In the case of a three-dimensional system of N *distinguishable* particles we substitute Eq. (12) into Eq. (30) and we again obtain Eq. (31) with

$$\epsilon_K=\frac{3Nn}{2}\,(1+k_{\max})\,\frac{1}{\beta}-\frac{\alpha}{\beta},$$

$$\alpha=\sum_{j=1}^{n}\left[(\widetilde{q}_{j+1}-\widetilde{q}_j)^2+\sum_{k=1}^{k_{\max}}\frac{(k\pi)^2}{2}\,\widetilde{A}_{jk}^2\right], \tag{32$'$}$$

$$\epsilon_P=\frac{1}{n}\sum_{j=1}^{n}\int_0^1 V(q_j(\xi))d\xi=\frac{1}{\beta}\sum_{j=1}^{n}\int_0^1 \widetilde{V}(\widetilde{q}_j(\xi))d\xi. \tag{33$'$}$$

Averaging $\langle O\rangle$ means again Eq. (34), now with Z and H from Eq. (12), $H=\alpha+\beta\epsilon_P$ with α and ϵ_P from Eqs. (32′) and (33′); $\widetilde{q}_j$, $\widetilde{q}_j(\xi)$ and $\widetilde{A}_{jk}$ are the $3N$-dimensional vectors introduced in Sec. II B, and Σ_k in $\widetilde{q}_j(\xi)$ being limited by $k_{\max}$.

Now for the three-dimensional system of N *identical* particles (fermions) we start with the partition functions (17) and (19). Differentiation (30) now yields again Eq. (31) with Eq. (32′) for ϵ_K and with $\langle\alpha\rangle$ and $\langle\epsilon_P\rangle$, now determined by

$$\langle\alpha\rangle=Z^{-1}\sum_G a_G\int d\widetilde{\tau}\alpha_G e^{-H_G}, \tag{35}$$

$$\langle \epsilon_P \rangle = Z^{-1} \sum_G a_G \int d\tilde{\tau}\, \epsilon_{PG} e^{-H_G},$$

where $Z=\Sigma_G a_G \int d\tilde{\tau} e^{-H_G}$. Here

$$\alpha_G = \sum_{j=1}^{n}{}^{(G)} \left[(\tilde{q}_{j+1}-\tilde{q}_j)^2 + \sum_{k=1}^{k_{\max}} \frac{(k\pi)^2}{2} \tilde{A}_{jk}^2 \right], \tag{36}$$

$$\epsilon_{PG} = \frac{1}{n}\sum_{j=1}^{n}{}^{(G)} \int_0^1 V(q_j(\xi))d\xi = \frac{1}{\beta}\sum_{j=1}^{n}{}^{(G)} \int_0^1 \tilde{V}(\tilde{q}_j(\xi))d\xi \tag{37}$$

H_G (19) and $H_G=\alpha_G+\beta\epsilon_{PG}$. The meaning of $\Sigma^{(G)}$ is the same as in Eq. (19). For H (12), H_G (19), α (32a), α_G (36), ϵ_P (33′), ϵ_{PG} (37) we can write

$$H_G = H+\Delta H_G, \quad \alpha_G=\alpha+\Delta\alpha_G, \quad \epsilon_{PG}=\epsilon_P+\Delta\epsilon_{PG},$$

where

$$\Delta\alpha_G = [\tilde{q}_n - P_G(\tilde{q}_1)]^2 - (\tilde{q}_n-\tilde{q}_1)^2,$$

$$\Delta\epsilon_{PG} = \int_0^1 V[q_n^G(\xi)]d\xi - \int_0^1 V[q_n(\xi)]d\xi,$$

$$\Delta H_G = \Delta\alpha_G + \beta\Delta\epsilon_{PG}.$$

Then Eq. (30) yields

$$E=\langle \epsilon_K \rangle + \langle \Delta\epsilon_K^{\text{exch}} \rangle + \langle \epsilon_P \rangle + \langle \Delta\epsilon_P^{\text{exch}} \rangle, \tag{38}$$

where ϵ_K and ϵ_P are determined as before by Eqs. (32a) and (33a); and for $\Delta\epsilon_K^{\text{exch}}$, $\Delta\epsilon_P^{\text{exch}}$ we have

$$\Delta\epsilon_K^{\text{exch}} = (\beta W)^{-1} \sum_G a_G \Delta\alpha_G e^{-\Delta H_G}, \tag{39}$$

$$\Delta\epsilon_P^{\text{exch}} = W^{-1} \sum_G a_G \Delta\epsilon_{PG} e^{-\Delta H_G}, \quad W=\sum_G a_G e^{-\Delta H_G}. \tag{40}$$

Averaging $\langle O \rangle$ in Eq. (38) implies

$$\langle O \rangle = Z^{-1} \int d\tilde{\tau} O e^{-H} W, \quad Z=\int d\tilde{\tau} e^{-H} W. \tag{41}$$

The average (38) can also be presented in symmetrical form

$$E=\langle \epsilon_K \rangle + \langle \Delta\epsilon_{Ks}^{\text{exch}} \rangle + \langle \epsilon_P \rangle + \langle \Delta\epsilon_{Ps}^{\text{exch}} \rangle \tag{38′}$$

with ϵ_K and ϵ_P determined, as in Eq. (38), by Eqs. (32′), (33′), and where

$$\Delta\epsilon_{Ks}^{\text{exch}} = (\beta W)^{-1} \sum_G a_G \frac{1}{n} \sum_{1\leqslant j\leqslant n} \Delta\alpha_G^{(j)} e^{-\Delta H_G^{(j)}}, \tag{39′}$$

$$\Delta\epsilon_{Ps}^{\text{exch}} = W^{-1} \sum_G a_G \frac{1}{n} \sum_{1\leqslant j\leqslant n} \Delta\epsilon_{PG}^{(j)} e^{-\Delta H_G^{(j)}}$$

$$W=\sum_G a_G \frac{1}{n} \sum_{1\leqslant j\leqslant n} e^{-\Delta H_G(j)} \tag{40′}$$

with

$$\Delta\alpha_G^{(j)} = [\tilde{q}_j - P_G(\tilde{q}_{j+1})]^2 - (\tilde{q}_j-\tilde{q}_{j+1})^2,$$

$$\Delta\epsilon_{PG}^{(j)} = \int_0^1 V[q_j^G(\xi)]d\xi - \int_0^1 V[q_j(\xi)]d\xi,$$

and

$$\Delta H_G^{(j)} = \Delta\alpha_G^{(j)} + \beta\Delta\epsilon_{PG}^{(j)}.$$

W and $\Delta H_G^{(j)}$ were already determined by Eq. (23) in Sec. II C.

$\Delta\epsilon_{Ks}^{\text{exch}}$ and $\Delta\epsilon_{Ps}^{\text{exch}}$ are expressed in Eqs. (39′) and (40′) in symmetrized form (see Sec. II C). Averaging $\langle O \rangle$ in this case implies Eq. (41) with W from Eq. (40′) [see also Eqs. (21), (22), (23)].

In the last two cases the integrand in the partition function Z (21) includes, in addition to the positive weight factor e^{-H}, the factor W which can change its sign. In order to apply MC important sampling (41) should be transformed into an expression including averages over positive weight function

$$\langle O \rangle = Z^{-1} \int d\tilde{\tau} O W e^{-H} = \frac{\int d\tilde{\tau} O \operatorname{sgn}(W)|W|e^{-H}}{\int d\tilde{\tau} \operatorname{sgn}(W)|W|e^{-H}} \times \frac{\int d\tilde{\tau}\, |W|e^{-H}}{\int d\tilde{\tau}\, |W|e^{-H}} = \frac{\langle O \operatorname{sgn}(W)\rangle_+}{\langle \operatorname{sgn}(W)\rangle_+}. \tag{42}$$

Here $\langle(\cdots)\rangle_+$ means

$$\langle(\cdots)\rangle_+ = \frac{\int d\tilde{\tau}(\cdots)|W|e^{-H}}{\int d\tilde{\tau}|W|e^{-H}}, \tag{43}$$

an averaging procedure with non-negative normalized weight function $|W|e^{-H}/\int d\tilde{\tau}\, |W|e^{-H}$ which now can be carried out within Metropolis procedure.

B. Virial estimator

In the same way as it has been done in [14] in ‘‘pure bead’’ PIMC method we can construct a virial estimator for the kinetic energy within the bead-Fourier approach. Starting again with the case $N=1$; $d=1$ we introduce the following linear operator $\hat{L}$:

$$\hat{L} = \sum_{j=1}^{n} \left(\tilde{x}_j \frac{\partial}{\partial \tilde{x}_j} + \sum_{k=1}^{k_{\max}} \tilde{a}_{jk} \frac{\partial}{\partial \tilde{a}_{jk}} \right). \tag{44}$$

Applying the $\hat{L}$ operator to H from Eq. (11) we construct canonical average $\langle \hat{L}H \rangle$ according to Eq. (34). Each of

$n(1+k_{\max})$ terms in the sum $\hat{L}$, e.g., $\tilde{x}_j(\partial/\partial\tilde{x}_j)$, or $\tilde{a}_{jk}(\partial/\partial\tilde{a}_{jk})$, being applied to H with subsequent averaging (34) yields 1 [14]. So we get

$$\langle\hat{L}H\rangle=n(1+k_{\max}). \tag{45}$$

As far as for H (11) we have $H=\alpha+\beta\epsilon_P$, where α and ϵ_P are Eqs. (32) and (33), we can write

$$\langle\hat{L}H\rangle=\langle\hat{L}\alpha\rangle+\beta\langle\hat{L}\epsilon_P\rangle=n(1+k_{\max}). \tag{46}$$

Note that α (32) is a quadratic form of Fourier amplitudes $\tilde{a}_{jk}$ and a cyclic sum of terms $(\tilde{x}_{j+1}-\tilde{x}_j)^2$. So it provides $\hat{L}\alpha=2\alpha$ and Eq. (46) yields

$$2\langle\alpha\rangle+\beta\langle\hat{L}\epsilon_P\rangle=n(1+k_{\max}),$$

or

$$\frac{1}{2}\langle\hat{L}\epsilon_P\rangle=\frac{n}{2\beta}(1+k_{\max})-\frac{1}{\beta}\langle\alpha\rangle. \tag{47}$$

The right side of Eq. (47) is the kinetic energy [see Eqs. (31) and (32)]. So it can be now expressed as an average of the virial estimator $\epsilon_K^{(v)}$

$$\langle\epsilon_K^{(v)}\rangle=\left\langle\frac{1}{2}\hat{L}\epsilon_P\right\rangle=\left\langle\sum_{j=1}^{n}\left(\tilde{x}_j\frac{\partial\epsilon_P}{\partial\tilde{x}_j}+\sum_{k=1}^{k_{\max}}\tilde{a}_{jk}\frac{\partial\epsilon_P}{\partial\tilde{a}_{jk}}\right)\right\rangle. \tag{48}$$

For N distinguishable particles, $d=3$, with similar steps we can arrive at

$$\langle\epsilon_K^{(v)}\rangle=\frac{1}{2}\langle\hat{L}\epsilon_P\rangle,\quad \hat{L}=\sum_{j=1}^{n}\left(\tilde{q}_j\frac{\partial}{\partial\tilde{q}_j}+\sum_{k=1}^{k_{\max}}\tilde{A}_{jk}\frac{\partial}{\partial\tilde{A}_{jk}}\right). \tag{49}$$

And finally we consider the case of N indistinguishable particles, $d=3$. Using the expression for partition functions (17), (19) we can introduce $\hat{L}H$ with $\hat{L}$ (49) and the average $\langle\hat{L}H\rangle$

$$\begin{aligned}\langle\hat{L}H\rangle&=Z^{-1}\sum_G a_G\int d\tilde{\tau}(\hat{L}H_G)e^{-H_G}\\&=3Nn(1+k_{\max})\frac{\sum_G a_G\int d\tilde{\tau}e^{-H_G}}{\sum_G a_G Z_D(G)}\\&=3Nn(1+k_{\max}).\end{aligned} \tag{50}$$

Here H_G is determined by Eq. (19), α_G is Eq. (36), ϵ_{PG} is Eq. (37), and $H_G=\alpha_G+\beta\epsilon_{PG}$ (see Sec. III A).

As far as $H=\alpha+\beta\epsilon_P$ with Eqs. (32a) and (33a) for α and ϵ_P

$$\langle\hat{L}H\rangle=\langle\hat{L}\alpha\rangle+\beta\langle\hat{L}\epsilon_P\rangle=3Nn(1+k_{\max}). \tag{51}$$

Now as far as α_G in Eq. (36) is again a quadratic form of Fourier amplitudes $\tilde{a}_{jk}$ and a cyclic sum of terms of the type $(\tilde{x}_{j+1}-\tilde{x}_j)^2$ we can show again that $\hat{L}\alpha=2\alpha$. If we substitute this into Eq. (51), take into account Eqs. (35), (32′), and (33′), we again obtain the virial estimator for the kinetic energy $\epsilon_K^{(v)}$

$$\epsilon_K^{(v)}=\tfrac{1}{2}\hat{L}\epsilon_P \tag{52}$$

with $\hat{L}$ from Eq. (49).

IV. EXACT RESULTS FOR A SYSTEM OF *N* NONINTERACTING IDENTICAL PARTICLES IN *D*-DIMENSIONAL OSCILLATOR FIELD

An exact expression of partition function for a system of N noninteracting spinless quantum identical particles in a one-dimensional $(d=1)$ oscillator field was derived in [15]

$$Z_N^{(A,S)}=\left[\prod_{1\leq l\leq N}\left(2\sinh\frac{l\beta}{2}\right)e^{\pm[N(N-1)/4]\beta}\right]^{-1}, \tag{53}$$

where A (antisymmetrical) and the upper sign refer to spinless fermions (‘‘polarized electrons’’) and S (symmetrical) and the lower sign refer to bosons. The corresponding expression for N distinguishable particles is well known

$$Z_N^{(D)}=(Z_1)^N=\left(2\sinh\frac{\beta}{2}\right)^{-N}, \tag{54}$$

where Z_1 is a single particle canonical partition function (in all that follows we use β instead of $\beta\hbar\omega$, i.e., consider $\hbar=\omega=1$). Expression (53) for $Z_N^{(A,S)}$ is easily derived if $d=1$, $sp=0$ [15] though its obtaining in similar cases for $d=2,3$ and $sp=1/2$ is not straightforward. The analysis of these cases that follows is based on the general expression for $Z_N^{(A,S)}$ (15), (17)

$$\begin{aligned}Z_N^{(A,S)}&=\frac{1}{N!}\sum_P \xi^{[P]}K(P)Z_N^{(D)}(P)\\&=\frac{1}{N!}\sum_G \xi^{[G]}K(G)n(G)Z_N^{(D)}(G).\end{aligned} \tag{55}$$

To be specific we start with $N=2$

$$Z_2^{(A,S)}=\tfrac{1}{2}[K(1^2)Z_2^{(D)}(1^2)\mp K(2)Z_2^{(D)}(2)]. \tag{56}$$

Here two classes of permutations for $N=2$ are designated as 1^2 and 2 and $n(1^2)=n(2)=1$ [16].

For a d-dimensional harmonic oscillator field (56) yields

$$Z_2^{(A,S)}(d,sp)=\tfrac{1}{2}[K(1^2)(Z_1^2)^d\mp K(2)(Z_2)^d], \tag{57}$$

where Z_1 is the partition function of a single particle in a one-dimensional case and Z_2 is the one for a cycle involving two particles $(d=1,\ sp=0)$. They are determined by the general expression for Z_ν derived in the Appendix, Eq. (A30)

$$Z_\nu=\frac{1}{2\sinh\dfrac{\nu\beta}{2}}. \tag{58}$$

For $sp=0$ $K(G)=1$ for all G; for $sp=1/2$ $K(1^2)=4$, $K(2)=2$ [2]. Now using Eq. (58) we present Eq. (57) in the following form:

$$Z_2^{(A,S)}(d,sp)=[Z_2^{(A,S)}]^d f_2(d,sp), \tag{59}$$

where $Z_2^{(A,S)}$ is a one-dimensional partition function, $sp=0$, determined by Eq. (53) for $N=2$ and

$$f_2(d,sp)=\frac{1}{2}\left[K(1^2)\left(\frac{2\sinh\beta e^{\pm(\beta/2)}}{2\sinh\frac{\beta}{2}}\right)^d \mp K(2)\left(2\sinh\frac{\beta}{2}e^{\pm[\beta/2]}\right)^d\right]. \tag{60}$$

For the antisymmetrical case and $sp=0$ $f_2(d,sp)$ can be presented as

$$f_2(d,sp=0)=\tfrac{1}{2}[(e^\beta+1)^d-(e^\beta-1)^d]. \tag{61}$$

So the corresponding partition function is

$$Z_2^{(A)}(d,sp=0)=(Z_2^{(A)})^d\times\begin{cases}1 & \text{for } d=1\\ 2e^\beta & \text{for } d=2\\ 3e^{2\beta}+1 & \text{for } d=3.\end{cases} \tag{62}$$

Similarly to Eq. (61) for the symmetrical case $(sp=0)$ we get

$$f_2(d,sp=0)=\tfrac{1}{2}[(1+e^{-\beta})^d+(1-e^{-\beta})^d] \tag{63}$$

and

$$Z_2^{(S)}(d,sp=0)=(Z_2^{(S)})^d\times\begin{cases}1 & \text{for } d=1\\ 1+e^{-2\beta} & \text{for } d=2\\ 1+3e^{-2\beta} & \text{for } d=3.\end{cases} \tag{64}$$

It should be noted that for $d=1$ in both cases we really obtain Eq. (53) for $N=2$.

Finally for fermions with $sp=1/2$ we have

$$f_2\left(d,sp=\frac{1}{2}\right)=\tfrac{1}{2}[4(e^\beta+1)^d-2(e^\beta-1)^d] \tag{65}$$

and

$$Z_2^{(A)}\left(d,sp=\frac{1}{2}\right)=(Z_2^{(A)})^d\times\begin{cases}e^\beta+3 & \text{for } d=1\\ e^{2\beta}+6e^\beta+1 & \text{for } d=2\\ e^{3\beta}+9e^{2\beta}+3e^\beta+3 & \text{for } d=3.\end{cases} \tag{66}$$

In all these cases the energy can be easily derived from $E=-(\partial/\partial\beta)(\ln Z)$. For antisymmetrical cases we can write (in $\hbar\omega$ units)

$$E_2^{(A)}(d,sp=0)=dE_2^{(A)}(d=1,\ sp=0)-\begin{cases}0 & \text{for } d=1\\ 1 & \text{for } d=2\\ \dfrac{6e^{2\beta}}{3e^{2\beta}+1} & \text{for } d=3\end{cases} \tag{67}$$

and

$$E_2^{(A)}\left(d,sp=\frac{1}{2}\right)=dE_2^{(A)}(d=1,\ sp=0)-\begin{cases}\dfrac{e^\beta}{e^\beta+3} & \text{for } d=1\\ \dfrac{2e^{2\beta}+6e^\beta}{e^{2\beta}+6e^\beta+1} & \text{for } d=2\\ \dfrac{3e^{3\beta}+18e^{2\beta}+3e^\beta}{e^{3\beta}+9e^{2\beta}+3e^\beta+3} & \text{for } d=3,\end{cases} \tag{68}$$

where $E_2^{(A)}(d=1,\,sp=0)$ is the energy of two particles with $sp=0$ in a one-dimensional oscillator field obtained from Eq. (53)

$$E_2^{(A)}(d=1,\ sp=0)=\tfrac{1}{2}\coth\frac{\beta}{2}+\coth\beta+\tfrac{1}{2}. \tag{69}$$

For a system of fermions with $sp=1/2$ we can calculate the value of the square of the total spin $\langle S(S+1)\rangle$. Using Eq. (29) and the coefficients from [2] we write

$$\langle S(S+1)\rangle^{(d)}=\frac{\frac{1}{2}[0\times1\times(1(Z_1^2)^d+1(Z_2)^d)+1\times2\times(3(Z_1^2)^d-3(Z_2)^d)]}{Z_2\left(d,sp=\frac{1}{2}\right)}. \tag{70}$$

Using Eqs. (62) and (66) we get

$$\langle S(S+1)\rangle=\begin{cases}\dfrac{6}{e^\beta+3} & \text{for } d=1\\ \dfrac{12e^\beta}{e^{2\beta}+6e^\beta+1} & \text{for } d=2\\ \dfrac{6(3e^{2\beta}+1)}{e^{3\beta}+9e^{2\beta}+3e^\beta+3} & \text{for } d=3.\end{cases} \tag{71}$$

As should be expected, in all cases $\langle S(S+1)\rangle$ tends to zero for $\beta\rightarrow\infty$ (spin compensation at low temperatures) and to $2\times\frac{3}{4}$ for $\beta\rightarrow0$ (a system of two independent ''classical'' electrons).

For a system of three particles $(N=3)$ the antisymmetrical partition function (55) can be represented similarly to Eq. (57) as

$$Z_3^{(A)}=\frac{1}{3!}\,[K(1^3)(Z_1^3)^d-3K(12)(Z_1Z_2)^d+2K(3)(Z_3)^d]. \tag{72}$$

Here $K_3(1^3)=8$, $K_3(12)=4$, and $K_3(3)=2$ for $sp=1/2$ [2]. Now, as in the previous case, we rewrite Eq. (72) in the form

$$Z_3^{(A)}(d,sp)=[Z_3^{(A)}]^d f_3(d,sp), \tag{73}$$

where $Z_3^{(A)}$ is Eq. (53) for $N=3$ and $f_3(d,sp)$ can be reduced [similarly to Eqs. (61) and (65)] to

$$f_3(d,sp)=\tfrac{1}{6}[(8)((e^{\beta}+1)(e^{2\beta}+e^{\beta}+1))^d-3(4)(e^{3\beta}-1)^d \\ +2(2)(e^{3\beta}-e^{2\beta}-e^{\beta}+1)^d]. \tag{74}$$

Here the additional coefficients 8, 4, and 2 are present only in the case $sp=1/2$. Finally for the partition function we obtain, for $sp=0$

$$Z_3^{(A)}(d,sp=0)=[Z_3^{(A)}]^d\times\begin{cases}1 \quad \text{for } d=1\\ e^{4\beta}+4e^{3\beta}+e^{2\beta} \quad \text{for } d=2\\ 3e^{7\beta}+10e^{6\beta}+6e^{5\beta}+6e^{4\beta}+7e^{3\beta}+3e^{2\beta}+1 \quad \text{for } d=3\end{cases} \tag{75}$$

and for $sp=1/2$

$$Z_3^{(A)}\left(d,sp=\frac{1}{2}\right)=[Z_3^{(A)}]^d\times\begin{cases}2(e^{2\beta}+e^{\beta}+2) \quad \text{for } d=1\\ 2e^{\beta}(2e^{4\beta}+5e^{3\beta}+10e^{2\beta}+5e^{\beta}+2) \quad \text{for } d=2\\ 2(3e^{8\beta}+12e^{7\beta}+29e^{6\beta}+30e^{5\beta}+30e^{4\beta}+23e^{3\beta}+12e^{2\beta}+3e^{\beta}+2) \quad \text{for } d=3.\end{cases} \tag{76}$$

The expressions for the energy and the value of the square of the total spin for $N=3$ are becoming rather long, so here we present them only for $d=1,3$ and $sp=1/2$ considering that all the rest can be easily derived similarly to Eqs. (67), (68), and (71). So

$$E_3^{(A)}\left(d,sp=\frac{1}{2}\right)=dE_3^{(A)}(d=1,\ sp=0)-\begin{cases}\dfrac{2e^{2\beta}+e^{\beta}}{e^{2\beta}+e^{\beta}+2} \quad \text{for } d=1\\ \dfrac{24e^{8\beta}+84e^{7\beta}+174e^{6\beta}+150e^{5\beta}+120e^{4\beta}+69e^{3\beta}+24e^{2\beta}+3e^{\beta}}{3e^{8\beta}+12e^{7\beta}+29e^{6\beta}+30e^{5\beta}+30e^{4\beta}+23e^{3\beta}+12e^{2\beta}+3e^{\beta}+2} \quad \text{for } d=3\end{cases} \tag{77}$$

and

$$\langle S(S+1)\rangle=\begin{cases}\dfrac{3}{4}\,\dfrac{e^{2\beta}+e^{\beta}+10}{e^{2\beta}+e^{\beta}+2} \quad \text{for } d=1\\ \dfrac{3}{4}\,\dfrac{3e^{8\beta}+36e^{7\beta}+109e^{6\beta}+78e^{5\beta}+78e^{4\beta}+79e^{3\beta}+36e^{2\beta}+3e^{\beta}+10}{3e^{8\beta}+12e^{7\beta}+29e^{6\beta}+30e^{5\beta}+30e^{4\beta}+23e^{3\beta}+12e^{2\beta}+3e^{\beta}+2} \quad \text{for } d=3.\end{cases} \tag{78}$$

For high temperatures ($\beta\rightarrow0$) $\langle S(S+1)\rangle$ tends to $\frac{3}{4}\times3$ (three independent particles) while for low temperatures ($\beta\rightarrow\infty$) it yields 3/4.

For greater number of particles ($N=4,5,\ldots$) analogous expressions can be obtained according to the same general scheme starting with formulas similar to Eqs. (57), (72), and (70). Though becoming more and more cumbersome these expressions can be easily obtained with the aid of the analytical programs (e.g., MATHEMATICA).

V. MC PROCEDURES AND PROGRAMMING

As a basis of simulations we used the partition functions in symmetrized form, (21) and (23) or (26) and (27) with the energy estimator (38′), (40′) (i.e., the primitive estimator for kinetic energy) and averaging according to Eqs. (41)–(43). For calculations of $\langle S(S+1)\rangle$ forms (26), (27), and (29) were used. Two independent programs were created: (1) in Pascal and (2) in *C* language.

In accord with the weight function in Eqs. (26) and (27) the MC random walk includes three main types of steps with attempts of: (1) Shift of an arbitrary bead j $(1\leqslant j\leqslant n)$ of an arbitrary particle i $(1\leqslant i\leqslant N)$; (2) change of an arbitrary Fourier amplitude a_{ijk} $(1\leqslant k\leqslant k_{\max})$; and (3) change of the spin S [trial of a new set of coefficients a_{GS} in Eq. (27)]. This point is performed simultaneously with the step of the first or the second kind. For better averaging, several additional types of steps were included as well: (4) move the whole trajectory of a particle by means of (a) parallel shift of all its beads; (b) rotation of the trajectory around one of the coordinate axes; (5) renumeration of particles which provides random walk inside classes. In the case of $N=3$, for instance, the class $G=\{12\}$ is initially represented by one of permutations (1–2, 3) the two others being accounted implicitly by the factor $n\{12\}=3$ (see Sec. II C and [2]); renumeration of particles enables us to include explicitly both other permutations—(1–3, 2) and (2–3, 1)—into averaging; and (6) cyclic renumeration of beads of a single randomly chosen particle; it results in variation of the exchange factor. Application of this algorithm seems to provide reliable sampling adequately covering significant areas of the space of states.

Simulations of an electronic system in the Coulomb field of nuclei creates a problem of potential singularity at $r=0$. It is resolved by smoothing of the electron-nucleus potential at short distances which is made in the usual way (e.g., [17,18]) substituting it either by a constant (a ‘‘shelf’’) or by another function which is finite at the origin. In most cases we used a parabolic smoothing

$$V_{\mathrm{eff}}(r)=\begin{cases} -\dfrac{e^2}{r} & \text{for } r>r_0 \\ ar^2+b & \text{for } r\leqslant r_0, \end{cases} \tag{79}$$

where r is an electron-nucleus distance, r_0 is the point of smooth ‘‘sewing together’’ the Coulomb function and the parabola with parameters $a=1/2(e^2/r_0^3)$, $b=-3/2(e^2/r_0)$, which provide continuity of the potential and its first derivative at r_0, b being the finite depth of Eq. (79) at the origin. The value of r_0 should be chosen small enough to make deviations of the results from those for the nonperturbed potential insignificant, but, at the same time, such that the ‘‘sinking’’ of the electron trajectory into a nucleus is prevented. The choice of r_0 is dependent on temperature, nucleus charge, and can be regulated by the number of beads and $k_{\max}$ (see Sec. VI). In test simulations for the ground state of the hydrogen atom we used $r_0=0.2$–0.3 of the Bohr radius.

The created programs allow us to perform a variety of simulations. It is possible to simulate systems with a different number of particles in the d-dimensional harmonic field, in a Coulomb field of a number of fixed nuclei, in cavities of different forms and size. As the input data, the following physical parameters are used: (1) the space dimension d; (2) the number of quantum particles N; (3) the number and positions of nuclei (while simulating Coulombic systems); (4) the value of r_0 in V_{eff} (in the same case); (5) the oscillator strength $\beta\hbar\omega$ (simulations in the oscillator field); (6) parameters of the cavity (simulations in a cavity); and (7) temperature.

Parameters of the MC procedure are the following: (1) the number of beads n; (2) the value of $k_{\max}$; (3) the number of MC steps; (4) the length of the initial interval of the chain to be truncated; and (5) the maximum shifts for steps of each kind (they are arranged so as to adjust the percentage of successful attempts to optimal values of 40–60%).

It is also possible to switch on or off: interaction between particles; the presence of a cavity with a different set of its parameters (the external potential); the exchange between particles. The integral in the potential part of the action was calculated at each step either by the simple trapezoidal rule (program 1) or by the Simpson method (program 2) with

TABLE I. BF-PIMC data for a system of N noninteracting identical particles ($sp=1/2$) in a d-dimensional harmonic field.

(a) $N=2$, $d=1$, N_{MC}[a]$=30\,000$					
β[b]	n[b]	$k_{\max}$[b]	$\langle E\rangle$[c]	$\langle S(S+1)\rangle$[c]	$\langle \mathrm{sgn}(W)\rangle_+$[c]
0.05	3	1	41.17 (2.2)[d]	1.48 (0.2)	0.991 (0.1)
0.25	3	1	8.34 (1.7)	1.40 (0.5)	0.951 (0.7)
0.5	3	1	4.31 (1.6)	1.29 (0.4)	0.901 (0.6)
1	3	1	2.38 (1.6)	1.06 (2.1)	0.779 (2.2)
1.5	3	1	1.76 (1.7)	0.80 (0.5)	0.760 (1.3)
2	5	1	1.39 (3.3)	0.56 (3.2)	0.657 (1.6)
2.5	5	2	1.25 (3.7)	0.39 (6.5)	0.640 (2.2)
3	5	2	1.15 (3.5)	0.24 (12)	0.567 (4.0)
3.5	6	2	1.07 (1.9)	0.13 (13)	0.614 (1.0)
4	7	2	1.02 (1.5)	0.11 (18)	0.625 (1.1)
5	7	2	0.99 (1.7)	0.08 (25)	0.671 (1.0)
(b) $N=2$, $d=3$, $N_{MC}=10\,000$					
β	n	$k_{\max}$	$\langle E\rangle$	$\langle S(S+1)\rangle$	$\langle \mathrm{sgn}(W)\rangle_+$
0.05	3	1	121.17 (3.3)	1.50 (0.1)	0.999 (0.1)
0.25	3	1	23.65 (2.8)	1.50 (0.3)	0.958 (0.1)
0.5	3	1	12.33 (2.6)	1.49 (0.3)	0.991 (0.2)
1	5	1	6.51 (2.5)	1.43 (1.5)	0.934 (2.0)
1.5	5	2	5.13 (5.4)	1.29 (3.1)	0.812 (3.3)
2	6	2	4.08 (8.0)	1.05 (4.9)	0.656 (5.1)
2.5	7	2	3.71 (8.2)	0.80 (5.4)	0.583 (5.8)
3	7	2	3.39 (5.9)	0.65 (1.2)	0.531 (4.4)
3.5	8	2	3.21 (7.3)	0.41 (8.1)	0.498 (5.3)
(c) $N=3$, $d=1$, $N_{MC}=100\,000$					
β	n	$k_{\max}$	$\langle E\rangle$	$\langle S(S+1)\rangle$	$\langle \mathrm{sgn}(W)\rangle_+$
0.05	3	1	59.14 (1.9)	2.19 (0.9)	0.945 (1.0)
0.25	3	1	12.84 (2.1)	1.97 (1.1)	0.788 (1.1)
0.5	3	1	6.88 (2.0)	1.75 (1.9)	0.638 (2.1)
1	3	1	3.99 (3.0)	1.24 (2.7)	0.410 (2.9)
1.5	3	2	3.16 (5.9)	1.06 (7.8)	0.244 (4.7)
2	5	2	2.84 (5.6)	0.85 (11)	0.158 (5.2)
2.5	5	2	2.71 (16)	0.77 (22)	0.105 (6.1)
3	6	2	2.54 (21)	0.68 (24)	0.051 (15)
3.5	6	2	2.35 (27)		0.036 (24)
4	7	2			0.029 (28)
(d) $N=3$, $d=3$, $N_{MC}=30\,000$					
β	n	$k_{\max}$	$\langle E\rangle$	$\langle S(S+1)\rangle$	$\langle \mathrm{sgn}(W)\rangle_+$
0.05	3	1	175.96 (2.6)	2.25 (0.3)	1.000 (0.1)
0.25	3	1	35.35 (3.0)	2.25 (0.3)	0.999 (0.1)
0.5	3	1	19.16 (2.5)	2.22 (0.9)	0.964 (1.2)
1	5	1	9.95 (4.1)	2.09 (2.7)	0.801 (4.2)
1.5	5	2	7.11 (11)	1.70 (4.1)	0.531 (9.8)
2	6	2	7.06 (14)	1.35 (15)	0.275 (10)
2.5	7	2	6.24 (15)	1.25 (23)	0.159 (14)
3	7	2	5.64 (25)	1.17 (32)	0.115 (20)
3.5	8	2	5.14 (31)		0.101 (26)

[a] N_{MC} is the number of Monte Carlo steps per a component, number of components is $Nn(1+k_{\max})$.

[b] Input parameters: β is the inverse temperature [in $(\hbar\omega)^{-1}$ units]; n is the number of beads; $k_{\max}$ is the number of Fourier coefficients.

[c] Output averages: $\langle E\rangle$ is the energy ($\hbar\omega$ units); $\langle S(S+1)\rangle$ is the square of total spin; $\langle \mathrm{sgn}(W)\rangle_+$ is the sign W [see Eqs. (23) and (27), Sec. II C and Eq. (43), Sec. III A].

[d] In each column the relative error in percent is given in parentheses.

TABLE II. BF-PIMC data for a system of N identical particles ($sp=1/2$) in a three-dimensional harmonic field at fixed $x=\beta\hbar\omega$ as a function of the electrostatic interaction parameter $y=C_q/C_h$.

(a) $N=2$, $x=1$, $n=3$, $k_{\max}=2$, $N_{MC}=30\,000$[a]				
y	$\langle E\rangle$	$\langle E_k\rangle$[b]	$\langle S(S+1)\rangle$	$\langle \mathrm{sgn}(W)\rangle_+$
0	6.52 (2.5)[c]	3.30 (4)	1.430 (1.5)	0.934 (2.0)
0.4	6.57 (3.4)	3.12 (7)	1.448 (0.6)	0.930 (0.8)
0.8	6.84 (1.6)	3.30 (2)	1.459 (0.5)	0.956 (0.7)
1.2	7.24 (3.0)	3.32 (4)	1.472 (0.4)	0.967 (0.9)
1.6	7.53 (3.5)	2.90 (5)	1.480 (0.4)	0.982 (0.6)
2.0	8.42 (2.2)	3.43 (3)	1.490 (0.2)	0.992 (0.2)
2.4	8.18 (2.2)	2.99 (6)	1.497 (0.2)	0.995 (0.3)
2.8	8.96 (1.8)	3.53 (2)	1.499 (0.2)	0.997 (0.2)
(b) $N=2$, $x=2$, $n=7$, $k_{\max}=2$, $N_{MC}=30\,000$				
y	$\langle E\rangle$	$\langle E_k\rangle$	$\langle S(S+1)\rangle$	$\langle \mathrm{sgn}(W)\rangle_+$
0	4.09 (8.0)	2.08 (11)	1.140 (4.9)	0.719 (5.1)
0.2	4.70 (4.2)	2.07 (5)	1.232 (3.0)	0.726 (3.3)
0.4	5.38 (4.3)	2.21 (10)	1.352 (3.5)	0.822 (3.8)
0.6	5.64 (2.5)	2.03 (6)	1.364 (2.3)	0.822 (2.6)
0.8	5.96 (4.2)	1.86 (5)	1.415 (2.3)	0.877 (2.8)
1	6.35 (2.2)	1.84 (7)	1.450 (1.2)	0.923 (1.5)
1.2	6.80 (2.8)	1.91 (9)	1.454 (1.6)	0.930 (2.1)
1.4	6.97 (1.6)	1.77 (7)	1.475 (0.9)	0.960 (1.2)
1.6	7.51 (1.9)	1.94 (7)	1.462 (1.5)	0.936 (2.0)
2	8.08 (1.4)	1.89 (6)	1.493 (0.5)	0.988 (0.6)
2.4	8.72 (1.1)	1.89 (5)	1.491 (0.7)	0.982 (0.9)
2.8	9.34 (1.4)	1.92 (6)	1.493 (1.1)	0.984 (1.5)
3.2	9.89 (1.0)	1.94 (5)	1.501 (0.1)	1.000 (0.1)
(c) $N=3$, $x=1$, $n=5$, $k_{\max}=1$, $N_{MC}=30\,000$				
y	$\langle E\rangle$	$\langle E_k\rangle$	$\langle S(S+1)\rangle$	$\langle \mathrm{sgn}(W)\rangle_+$
0	9.93 (4.1)	4.86 (5)	2.089 (2.7)	0.801 (1.2)
0.4	11.37 (4.9)	5.27 (5)	2.135 (2.9)	0.878 (3.6)
0.8	12.02 (1.7)	4.86 (4)	2.161 (1.2)	0.914 (1.5)
1.2	12.89 (1.2)	4.95 (3)	2.180 (1.6)	0.934 (1.9)
1.6	13.75 (1.2)	4.86 (4)	2.198 (1.0)	0.949 (1.2)
2.0	14.73 (1.7)	4.95 (5)	2.212 (1.0)	0.962 (1.3)
2.4	15.54 (0.8)	5.00 (2)	2.220 (0.9)	0.968 (1.2)
2.8	16.05 (0.8)	4.72 (3)	2.240 (0.1)	0.989 (0.3)

[a] Meanings of n, $k_{\max}$, N_{MC}, $\langle E\rangle$, $\langle S(S+1)\rangle$, $\langle \mathrm{sgn}(W)\rangle_+$ are the same as in Table I.

[b] $\langle E_k\rangle$ is average kinetic energy.

[c] In each column the relative error in percent is given in parentheses.

preliminary tabulation of the sine function. The number of integration points is bound with the value of $k_{\max}$.

Test simulations presented in Sec. VI were performed on two computers PC 486DX/2-66. Typical calculation time per each run, Figs. 1–8 and Tables I and II, ranged from 10–30 minutes for high temperature cases up to 3 to 4 hours for lowest temperatures studies.

VI. TEST RESULTS AND DISCUSSION

A. Single particle: an electron in the hydrogen atom and a particle in the harmonic field

To test the bead-Fourier PIMC method and to explore its facilities we started with the simplest case of a single particle in an external field within two models: (1) a charged particle in a three-dimensional Coulomb potential—a hydrogen atom, in this case we can reproduce its exact ground-state energy and the distribution function; (2) a particle in a one-dimensional harmonic field.

We simulated an electron in the electrostatic potential smoothed at short distances according to Eq. (79) with $r_0=0.2$–$0.3\ R_b$ ($R_b=0.53$ Å being the Bohr radius). In most of our runs we used temperature $T=10\,000$ K (about 1 eV) which is ten times less than the first gap in the hydrogen spectrum [$(1-1/4)$ 13.6 eV$=$10.2 eV). So we are sure to obtain almost pure ground-state energy $E_0=-13.6$ eV and the distribution function of the electron.

Convergence of the calculated energy to the exact ground-state level is demonstrated in Fig. 1. Figure 1(a) shows how the results attain the level E_0 in three series of BF-PIMC calculations ($T=10\,000$ K) for different fixed numbers of beads n with the increase of $k_{\max}$. It is evident that for $n=70$ $k_{\max}=3$ is already sufficient while for $n=50$ saturation is achieved only for $k_{\max}=4$; for $n=30$ even $k_{\max}=6$ is yet insufficient. For a lower temperature ($T=5000$ K) dependencies both for $n=30$ and 50 are far from saturation within the range of $k_{\max}\leqslant 6$. Analogous dependencies of $\langle E\rangle$ on the number of beads n for different fixed values of $k_{\max}$ [Fig. 1(b)] are also instructive in making choice of the optimal set of parameters n and $k_{\max}$. It is seen that $k_{\max}=3$ provides practical identity of results for $n\geqslant 40$ while for $k_{\max}=1$ the level E_0 is not achieved even for $n=80$. Figure 2 demonstrates a good reproduction of the exact electron density distribution function in the ground state ($\rho(r)=(1/\pi R_b^3)\exp(-[2r/R_b])$) in calculations with the optimal set of input free parameters n and $k_{\max}$.

Figure 3 shows convergence of the calculated energy to the exact dependence ($E_0=1/2\coth\beta/2$) with the increase of $k_{\max}$ for different reduced temperatures and the number of beads for the quantum oscillator. It is seen that lower temperatures and smaller number of beads require higher values of $k_{\max}$ for saturation to the desired level. The optimal combination of n and $k_{\max}$ for each inverse temperature can be readily determined from such plots.

It should be noted again that $k_{\max}=0$ corresponds to ‘‘pure bead’’ method with the only difference that in this case the potential source is homogeneously distributed along the interval between two beads while in the ‘‘initial’’ bead method (as it is treated in most papers) the potential is centered on beads. The continuous distribution variant is certainly better for PIMC computations. Though even in this case, as we can see in Fig. 1(a), $n=70$ is far from being sufficient to reproduce correctly E_0 for H atom. On the other hand ‘‘pure Fourier’’ procedure means in our terms that $n=1$. Looking at Figs. 1(a) and 1(b) it is not easy to imagine how great is the number of Fourier components which could provide an adequate result in calculations with $n=1$. So, as it was mentioned in the Introduction, ‘‘pure bead’’ and ‘‘pure Fourier’’ procedures as being the extreme cases of our combined approach are far from the optimal simulation regime.

B. Several noninteracting identical particles with $sp=1/2$ in harmonic field

We use a favorable opportunity to check the quality of the developed procedures by comparison of simulation results

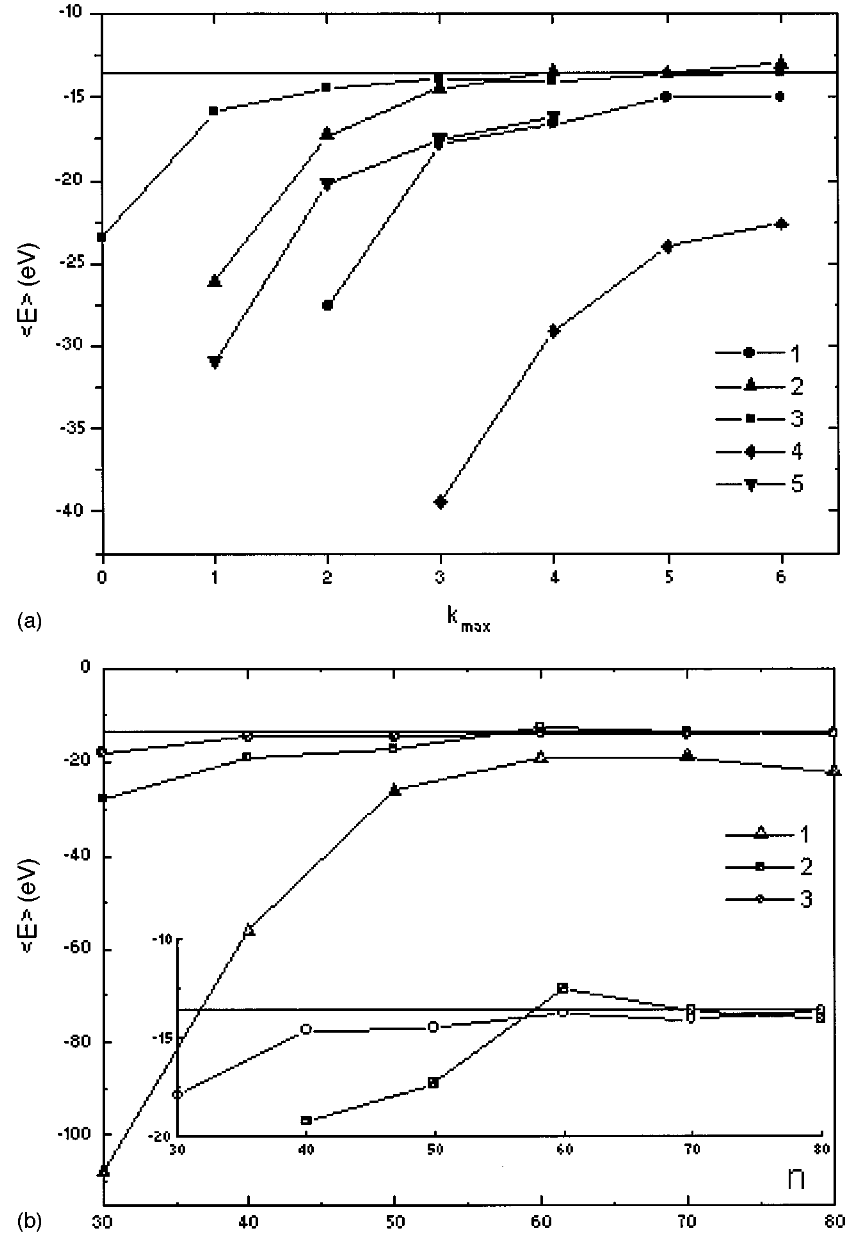

FIG. 1. Average energy of an electron in H atom from BF-PIMC simulations with a different number of beads n and number of Fourier components k_{max}. Horizontal line is the ground-state energy $E_0 = -13.6$ eV; (a) for various number of beads n and temperatures T as a function of k_{max}; values of n: 1−30, 2−50, 3−70 ($T = 10\,000$ K); 4−30, 5−50 ($T = 5000$ K); (b)—for various k_{max} at $T = 10\,000$ K as a function of the number of beads n; values of k_{max}: 1−1, 2−2, 3−3; (lines connecting points are drawn to guide the eye).

for systems of $N = 2$ and 3 identical particles with $sp = 1/2$ in a d-dimensional harmonic field with the exact dependencies derived in Sec. IV (Figs. 4–6, Table I).

Simulation data for $N = 2$ versus inverse temperature for canonical energy and average square of the total spin are presented in Figs. 4(a) and 5(a), corresponding exact dependencies are shown by solid lines. For the energy we observe almost perfect reproduction of the exact curves in a wide temperature range up to the ground-state levels for both dimensions, $d = 1$ and 3. For $\langle S(S+1)\rangle$ the coincidence is also good though for high β the statistical errors increase considerably (see Table I). For $\langle \mathrm{sgn}(W)\rangle_+$ [Fig. 6(a)] there exists no exact expression to be compared with simulation results. The general feature of observed dependencies is their decrease with the increase of β though, even for highest β, values of $\langle \mathrm{sgn}(W)\rangle_+$ do not fall lower than 0.6 for $d = 1$ and 0.4 for $d = 3$. So, as it could be expected from general considerations, for $N = 2$, $sp = 1/2$ the sign problem does not yet arise.

Analogous data for $N = 3$ are presented in Figs. 4(b), 5(b), 6(b). In this case the decrease of $\langle \mathrm{sgn}(W)\rangle_+$ with the growth of β is much stronger [Fig. 6(b)]. Thus for $\beta = 3$–4 values of $\langle \mathrm{sgn}(W)\rangle_+$ are already either equal to 0.1 (for $d = 3$) or less than 0.1 (for $d = 1$). So for $N = 3$ the sign problem already emerges. Nevertheless, E dependencies on β [Fig. 4(b)] are reproduced in BF-PIMC simulations almost as accurately as for $N = 2$ [Fig. 4(a)]. For $\langle S(S+1)\rangle$ accuracy of results are good for $\beta \leqslant 2.5$ ($d = 1$) and for $\beta \leqslant 2$ ($d = 3$). In the latter case for higher β the error becomes great (see Table I) and we get a considerable scatter of MC results.

C. Several identical particles, $sp = 1/2$, with electrostatic repulsion in harmonic field

The effect of gradual switching on of the electrostatic repulsion between particles in the above considered model (N identical particles in the harmonic field) is revealed in Figs. 7, 8, and Table II.

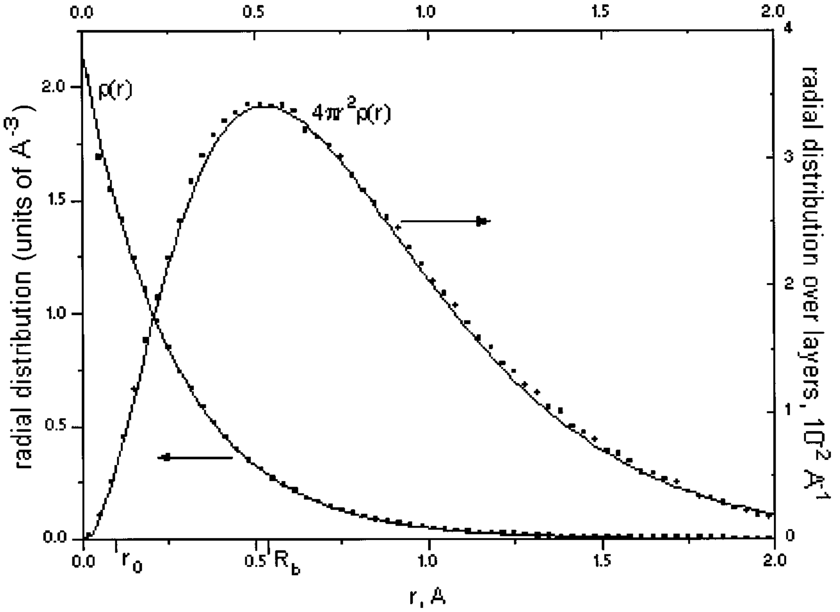

FIG. 2. Electron density distribution function in H atom. Solid lines are exact dependencies: $1-\rho(r)=(1/\pi R_b^3)\exp(-[2r/R_b])$; $2-4\pi r^2\rho(r)$. Points are corresponding BF-PIMC distributions obtained at $T=10\,000$ K for $n=70$, $k_{\max}=6$, $r_0=0.2\ R_b$ [see Fig. 1(a)].

The parameter which determines the ratio of electrostatic interaction to the harmonic field intensity is $y=C_q/C_h$ where $C_q=e^2/\Lambda$; $C_h=m\omega^2\Lambda^2/2$, Λ being the thermal wavelength. Finally we get

$$y=\frac{e^2}{h}\sqrt{\frac{2m}{\pi}}\frac{1}{x^2}\sqrt{\beta},$$

where $x=\beta\hbar\omega$, $\beta=(kT)^{-1}$. So for each fixed x and y (if e and m are the charge and the mass of an electron) we can obtain the temperature in Kelvin.

We performed three series of simulations each with fixed x and gradual increase of y. Figures 7 and 8 demonstrate how $\langle S(S+1)\rangle$ and $\langle \mathrm{sgn}(W)\rangle_+$ starting with their values for a system of noninteracting particles (Table I, Figs. 5 and 6) tend to their ''classical'' levels as the electrostatic repulsion is being switched on. Correspondingly the total energy (Table II) monotonously increases while the kinetic energy practically remains constant.

VII. CONCLUDING REMARKS

In this paper the combined, bead-Fourier, variant of the PIMC method was formulated and relevant expressions for partition functions and canonical averages were derived both for systems of distinguishable and identical particles. ''Pure bead'' and ''pure Fourier'' methods are the extreme cases of our combined approach and appear to be nonoptimal compared with the latter. In the case of identical particles forms symmetrical with respect to exchange were introduced; other forms of the partition function with explicit averaging over the square of the total spin or its projection were obtained as

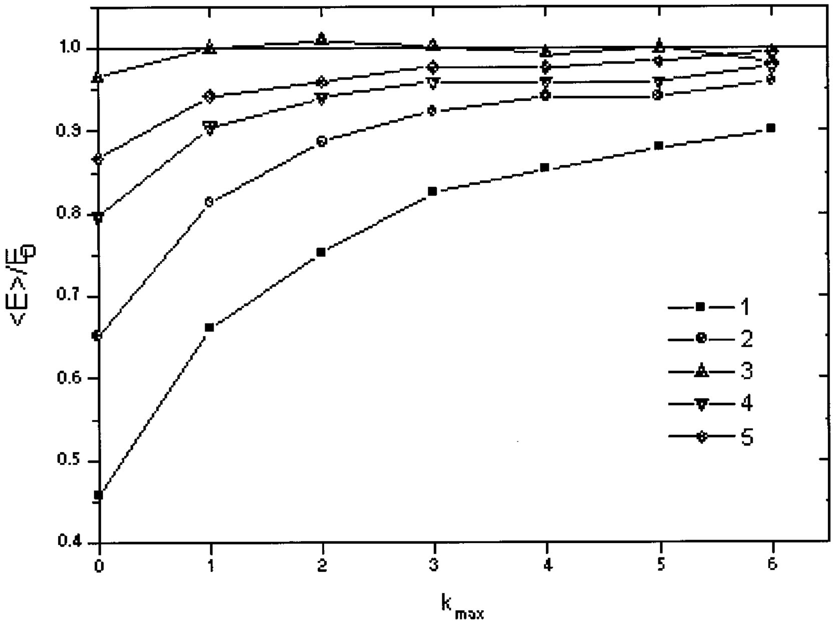

FIG. 3. Average energy of a single particle in one-dimensional harmonic field in E_0 units ($E_0=1/2\coth\beta/2$ is the exact dependence) as a function of $k_{\max}$ for different values of inverse reduced temperature β and the number of beads n; values of β and n: $1-10$ (3), $2-5$ (3), $3-1$ (3), $4-5$ (6), $5-5$ (10); (lines connecting points are to guide the eye).

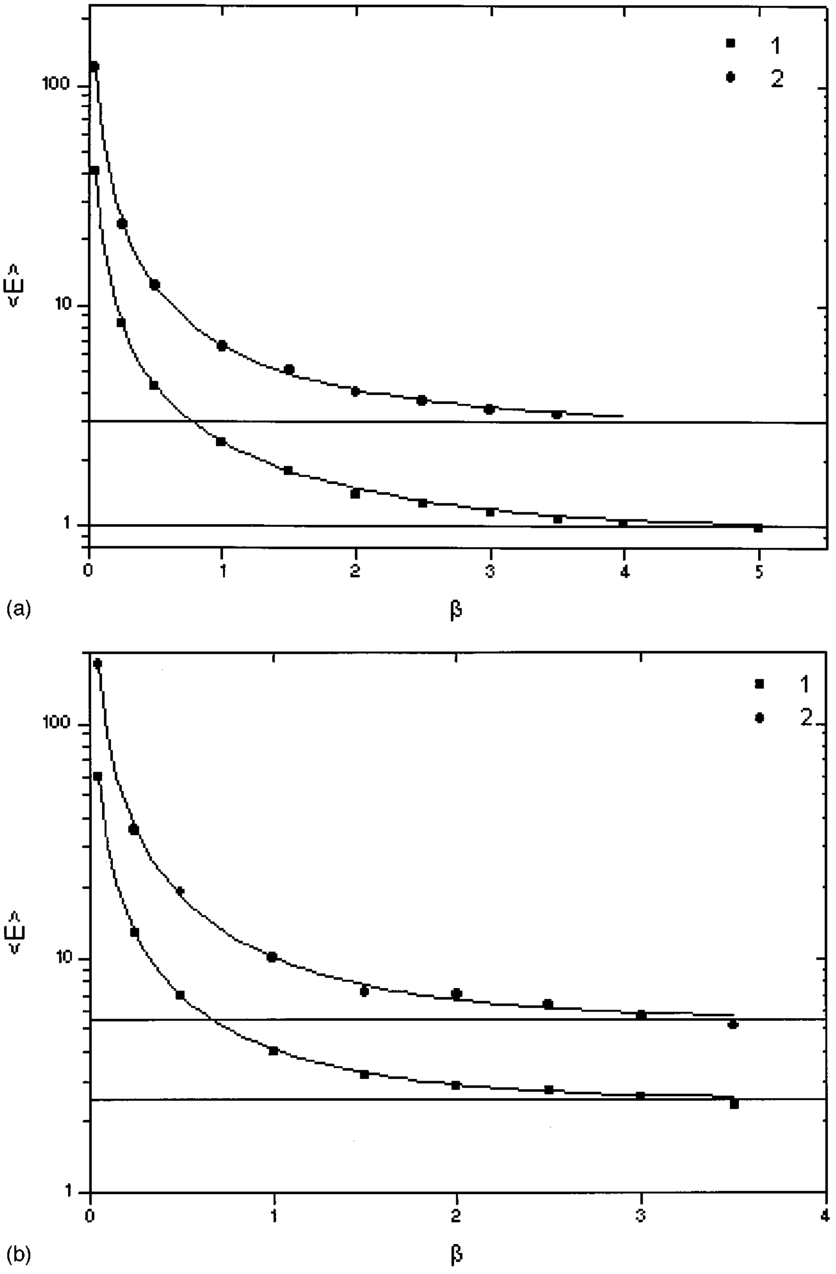

FIG. 4. β dependency of the average energy ($h\omega$ units) for a system of N noninteracting identical particles ($sp=1/2$) in d-dimensional harmonic field. (a)—$N=2$; (b)—$N=3$. $1-d=1$; $2-d=3$. Solid lines are exact dependencies (68) for (a) and (77) for (b), Sec. IV. Horizontal lines mark ground states: $E_{1gs}=1$, $E_{3gs}=3$ for (a) and $E_{1gs}=2.5$, $E_{3gs}=5.5$ for (b).

well. Relevant algorithms and computer programs, created on the basis of the suggested approaches, were tested by comparing simulation results with exact data, both for a single particle in the external field (H atom, harmonic oscillator) and a model system of $N=2,3$ identical noninteracting particles in the harmonic field. To carry out such comparison we derived exact β dependencies of canonical averages for the system of noninteracting identical particles with spin in a d-dimensional harmonic field. The comparison indicates that the developed approaches and simulation procedures give reliable results in a wide β range up to rather low relative temperatures ($\beta \leqslant 3-4$). Simulations with switching on of the electrostatic repulsion between particles in the harmonic field demonstrate gradual removal of the exchange effects. The attractive feature of the developed BF-PIMC method is that for each simulated quantum system it is possible to determine the optimal computational regime by an appropriate choice of the number of beads and value of $k_{\max}$. The results obtained in this work provide certain optimism in further attack on finite temperature simulations of systems including electrons such as dense plasma, electrides, metallic microdrops in zeolites, etc. The BF method can also be useful in PIMC simulations of heavy quantum particle systems when the exchange effects are usually neglected.

ACKNOWLEDGMENTS

This work has been supported by the Russian Foundation of Fundamental Research, Grant No. 96-03-33856a. We are also very grateful to Professor Victor F. Ossipov for his aid in the treatment of some mathematical issues in the Appendix.

APPENDIX

1. A single particle in one dimension

Our first step is to show that in the case of the one-dimensional harmonic potential $V(x)=(m\omega^2/2)x^2$ the parti-

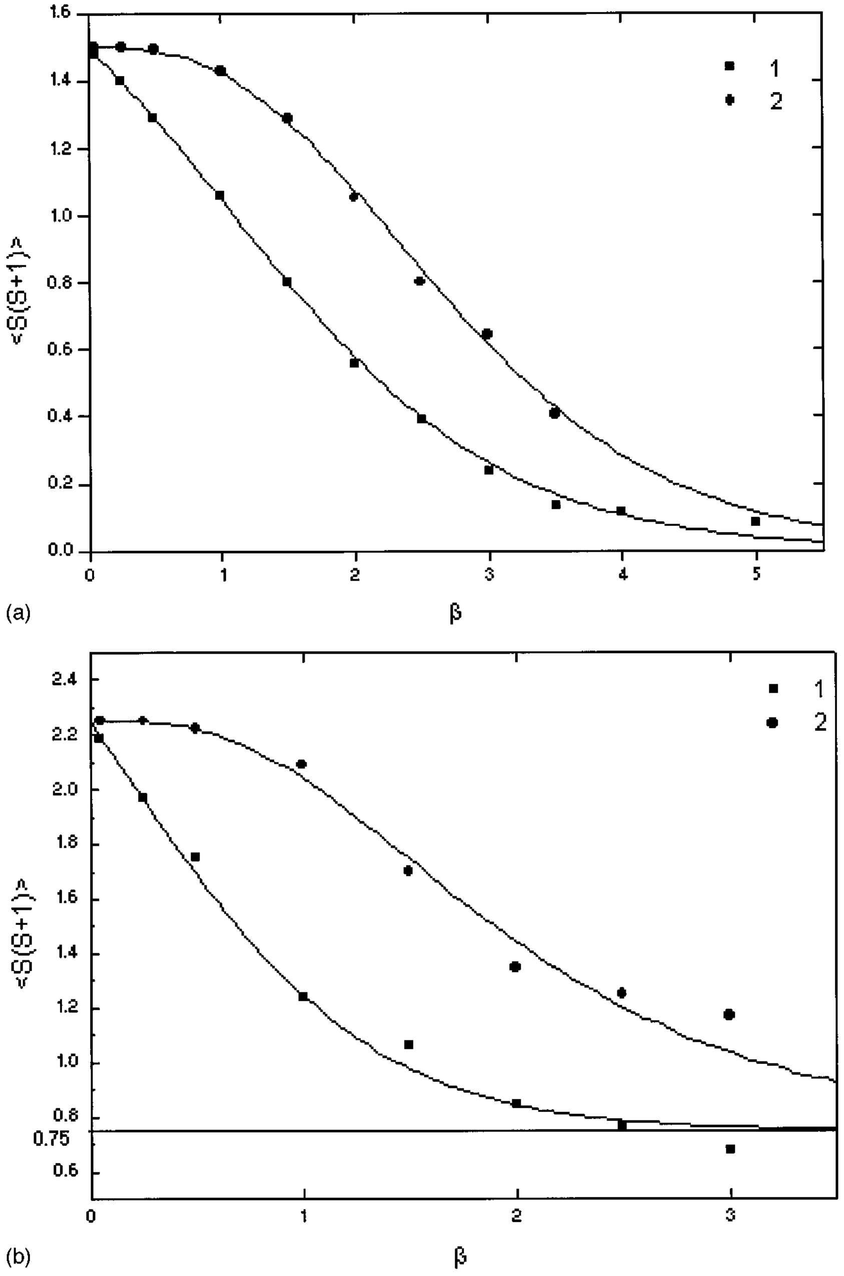

FIG. 5. β dependency of the average square of total spin for the same systems as in Fig. 4. (a)—$N=2$; (b)—$N=3$. $1-d=1$; $2-d=3$. Solid lines are exact dependencies (71) for (a) and (78) for (b), Sec. IV. Horizontal line in (b) is the ground-state level.

tion function for a single particle, Eq. (11), yields $Z_1=[2\sinh(\beta/2)]^{-1}$. The easiest way to do so is to use expression (11) in a purely Fourier form (i.e., the number of beads $n=1$)

$$Z_1=\int\frac{1}{\sqrt{\pi}}\,d\widetilde{x}\prod_{k=1}^{\infty}\frac{\pi k}{\sqrt{2\pi}}\,d\widetilde{a}_k \times\exp\left[-\left(\sum_{k=1}^{\infty}\frac{(k\pi)^2}{2}\,\widetilde{a}_k^{\,2}+\int_0^1\widetilde{V}[\widetilde{x}(\xi)]d\xi\right)\right], \tag{A1}$$

where the potential now is

$$\widetilde{V}[\widetilde{x}(\xi)]=\beta\,\frac{m\omega^2}{2}\,\text{unit}^2[\widetilde{x}(\xi)]^2=(\beta\hbar\omega)^2\widetilde{x}^{\,2}(\xi)$$

and

$$\widetilde{x}(\xi)=\widetilde{x}+\Sigma_k\widetilde{a}_k\sin k\pi\xi.$$

Its integration yields

$$\int_0^1\widetilde{V}[\widetilde{x}(\xi)]d\xi=(\beta\hbar\omega)^2\left(\widetilde{x}^{\,2}+2\widetilde{x}\sum_k\,\widetilde{a}_kf_k+\sum_k\,\frac{\widetilde{a}_k^{\,2}}{2}\right),$$

where

$$f_k=\int_0^1 \sin k\pi\xi d\xi=\frac{1}{k\pi}\,[1-(-1)^k]. \tag{A2}$$

From here to the conclusion of the Appendix we omit tildes over x and a_k and use β instead of $\beta\hbar\omega$. The exponent term in (A1) now becomes

$$\exp\left[-\left(\sum_k\,(B_k a_k^2+\beta^2 a_k f_k 2x)+\beta^2 x^2\right)\right],$$

where

$$B_k=\frac{\beta^2+(k\pi)^2}{2}. \tag{A3}$$

It can be transformed into

$$\exp\left[-\left(\sum_k\,(a_k\sqrt{B}_k+xC_k)^2+\alpha x^2\right)\right],$$

$$\alpha=\beta^2-\sum_k\,C_k^2,\quad C_k=\frac{\beta^2 f_k}{\sqrt{B}_k}. \tag{A4}$$

So the partition function becomes a product of Gauss integrals, internal infinite product I_1 and external one-dimensional integral I_2

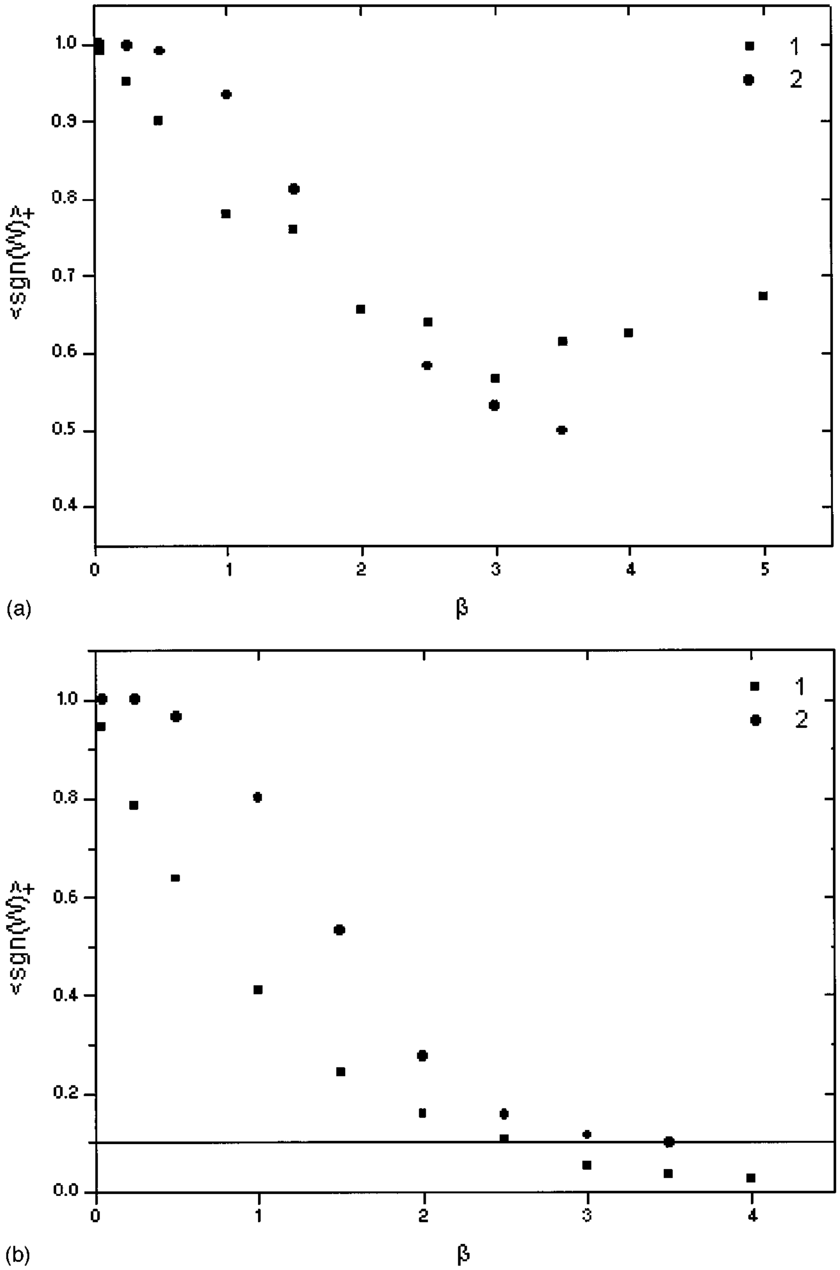

FIG. 6. β dependency of the average sign of W for the same systems as in Figs. 4, 5. Horizontal line in (b) marks the 0.1 level.

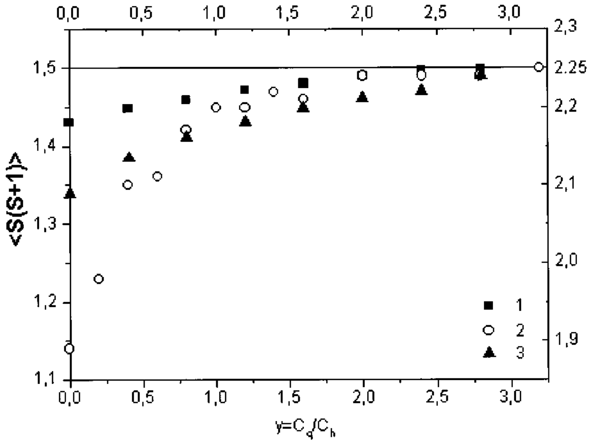

FIG. 7. Average of the square of the total spin vs y for a system of N identical particles ($sp=1/2$) with Coulomb interaction in three-dimensional harmonic field with fixed $x=\beta\hbar\omega$: $1-N=2$, $x=1$; $2-N=2$, $x=2$; $3-N=3$, $x=1$.

$$I_1=\prod_{k=1}^{\infty}\int_{-\infty}^{\infty}\frac{\pi k}{\sqrt{2\pi}}\,da_k\exp[-(a_k\sqrt{B}_k+xC_k)^2]$$

$$=\left[\prod_{k=1}^{\infty}\left(1+\frac{\beta^2}{(k\pi)^2}\right)\right]^{-1/2}=\left(\frac{\beta}{\sinh\beta}\right)^{1/2}. \qquad \text{(A5)}$$

The infinite product here is reduced to a sinh β function according to [19], Chap. 1, No. 1.431.2. Note also that the result, Eq. (A5), is independent of x. So

$$I_2=\int_{-\infty}^{\infty}\frac{dx}{\sqrt{\pi}}\exp(-\alpha x^2)=\frac{1}{\sqrt{\alpha}}. \qquad \text{(A6)}$$

For α we have from Eqs. (A4), (A3), and (A2)

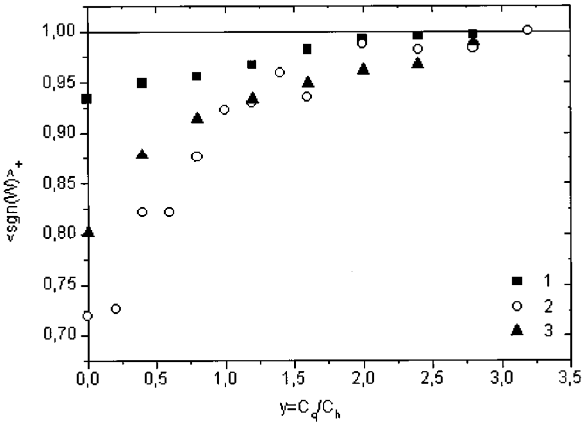

FIG. 8. y dependency for $\langle\text{sgn}(W)\rangle_+$, the system and designations are the same as in Fig. 7.

$$\alpha=\beta^2\left(1-\beta^2\sum_{n=1}^{\infty}\frac{8}{(2n-1)^2\pi^2[(2n-1)^2\pi^2+\beta^2]}\right)$$

$$=\beta^2\left[1-8\left(\frac{1}{\pi^2}\sum_{n=1}^{\infty}\frac{1}{(2n-1)^2}-\sum_{n=1}^{\infty}\frac{1}{(2n-1)^2\pi^2+\beta^2}\right)\right]$$

$$=\beta^2\left[1-8\left(\frac{1}{\pi^2}\frac{\pi^2}{8}-\frac{\tanh\left(\frac{\beta}{2}\right)}{4\beta}\right)\right]=2\beta\tanh\left(\frac{\beta}{2}\right) \qquad \text{(A7)}$$

(both sums are reduced according to [19], Chap. 0, No 0.234.2 and Chap. 1, No 1.421.2). Combining I_1 and I_2 we have finally for Z_1

$$Z_1=I_1I_2=\left(\frac{\beta}{\sinh(\beta)2\beta\tanh\left(\frac{\beta}{2}\right)}\right)^{1/2}=\left[2\sinh\left(\frac{\beta}{2}\right)\right]^{-1}. \qquad \text{(A8)}$$

2. *N* identical particles

In the case of N identical particles ($d=1$) we can start with Eqs. (15)–(19) using the pure Fourier form of Eq. (19) ($n=1$) for $Z_D(P)$

$$Z_D(P)=\int d\tau\exp\left[-\sum_{i=1}^{N}\left(\sum_{k=1}^{\infty}\frac{(k\pi)^2}{2}a_{ik}^2+[x-P(x_i)]^2+\int_0^1 V[x_i(\xi)]d\xi\right)\right]. \qquad \text{(A9)}$$

After integration of the potential the exponent in Eq. (A9) finally transforms into

$$\exp\left[-\sum_i\left(\sum_k B_ka_{ik}^2+[x_i-P(x_i)]^2+\frac{\beta^2}{3}\{x_i^2+[P(x_i)]^2+x_iP(x_i)\}+2\beta^2\left\{x_i\sum_k a_{ik}f_k+[P(x_i)-x_i]\sum_k a_{ik}g_k\right\}\right)\right]. \qquad \text{(A10)}$$

Here B_k and f_k are determined as in Eqs. (A3) and (A2) and $g_k=\int_0^1\xi\sin k\pi\xi d\xi=[-(-1)^k/k\pi]$.

For the identical permutation (1^N) it yields

$$\exp\left[-\sum_i\left(\sum_k(B_ka_{ik}^2+\beta^2a_{ik}f_k2x_i)+\beta^2x_i^2\right)\right]. \qquad \text{(A11)}$$

So Eq. (A9) becomes a product of N identical integrals (A1) and we finally obtain

$$Z_D(1^N)=(Z_1)^N=\left[2\sinh\left(\frac{\beta}{2}\right)\right]^{-N}. \qquad \text{(A12)}$$

In the general case (A10) we again arrive at separation of $Z_D(P)$ into Gauss integrals I_1 and I_2

$$I_1=\prod_{i=1}^{N}\prod_{k=1}^{\infty}\left(\int_{-\infty}^{\infty}\frac{k\pi}{\sqrt{2\pi}}\,da_{ik}\exp[-(a_{ik}\sqrt{B}_k+C_{ik})]\right), \tag{A13}$$

where now

$$C_{ik}=\beta^2\,\frac{x_i f_k+[P(x_i)-x_i]g_k}{\sqrt{B}_k}. \tag{A14}$$

I_1 does not depend on C_{ik} (and, hence, on coordinates x_i) and it yields the Nth power of Eq. (A5)

$$I_1=\left(\frac{\beta}{\sinh\beta}\right)^{N/2}.$$

It remains for us to calculate the integral I_2

$$I_2=\int\prod_{i=1}^{N}\frac{dx_i}{\sqrt{\pi}}\exp\left[-\sum_i\left(-\sum_k C_{ik}^2+[x_i-P(x_i)]^2+\frac{\beta^2}{3}\{x_i^2+[P(x_i)]^2+x_iP(x_i)\}\right)\right]. \tag{A15}$$

Transformation of the sum over k yields

$$\sum_k C_{ik}^2=\beta^4\left[x_i^2\sum_k\frac{(f_k-g_k)^2}{B_k}+[P(x_i)]^2\times\sum_k\frac{g_k^2}{B_k}+2x_iP(x_i)\sum_k\frac{(f_k-g_k)g_k}{B_k}\right]. \tag{A16}$$

As far as $g_k^2=(f_k-g_k)^2=(k\pi)^{-2}$ and $(f_k-g_k)g_k=(-1)^{k+1}(k\pi)^{-2}$, the sum, Eq. (A16), can be further transformed as

$$\begin{aligned}\sum_k C_{ik}^2&=\beta^4\left[[x_i^2+P(x_i)^2]\sum_k\frac{2}{(k\pi)^2[\beta^2+(k\pi)^2]}+2x_iP(x_i)\sum_k\frac{2(-1)^{k+1}}{(k\pi)^2[\beta^2+(k\pi)^2]}\right]\\&=2\beta^2\left[[x_i^2+P(x_i)^2]\left(\frac{1}{\pi^2}\sum_k\frac{1}{k^2}-\sum_k\frac{1}{\beta^2+(k\pi)^2}\right)+2x_iP(x_i)\left(\frac{1}{\pi^2}\sum_k\frac{(-1)^{k+1}}{k^2}-\sum_k\frac{(-1)^{k+1}}{\beta^2+(k\pi)^2}\right)\right]\\&=2\beta^2\left\{[x_i^2+P(x_i)^2]\left[\frac{1}{\pi^2}\frac{\pi^2}{6}-\left(\coth\beta-\frac{1}{\beta}\right)\frac{1}{2\beta}\right]+2x_iP(x_i)\left[\frac{1}{\pi^2}\frac{\pi^2}{12}+\left(\frac{1}{\sinh\beta}-\frac{1}{\beta}\right)\frac{1}{2\beta}\right]\right\}.\end{aligned} \tag{A17}$$

The sums in Eq. (A17) are reduced due to [19] Chap. 0, No. 0.233.3; Chap. 1, No. 1.421.4; Chap. 0, No. 0.234.1; Chap. 1, No. 1.217.2. Substituting this into Eq. (A15) we finally obtain for I_2:

$$I_2=\int\prod_{i=1}^{N}\frac{dx_i}{\sqrt{\pi}}\exp\left[-\frac{\beta}{\sinh\beta}\sum_i\{[x_i^2+P(x_i)^2]\cosh\beta-2x_iP(x_i)\}\right]. \tag{A18}$$

Now for $Z_D(P)$ we have

$$\begin{aligned}Z_D(P)&=I_1I_2\\&=\left(\frac{\beta}{\sinh\beta}\right)^{N/2}I_2\\&=\frac{1}{\pi^{N/2}}\int\prod_{i=1}^{N}dy_i\\&\quad\times\exp\left[-\sum_i\{C[y_i^2+P(y_i)^2]-2y_iP(y_i)\}\right].\end{aligned} \tag{A19}$$

Here

$$C=\cosh\beta,\quad y_i=\left(\frac{\beta}{\sinh\beta}\right)^{1/2}x_i.$$

Factor $I_1=(\beta/\sinh\beta)^{N/2}$ in Eq. (A19) is ‘‘consumed’’ by the new variable y_i.

For each permutation the integral $Z_D(P)$, Eq. (A19), evidently separates into a product over cycles,

$$Z_D(P)=Z_D(G)=\prod_{1\leqslant\nu\leqslant N}(Z_\nu)^{C_\nu(G)}.$$

So our aim is to calculate the integral (A19) for a single cycle of the length ν which we designate as Z_ν

$$Z_\nu=\frac{1}{\pi^{\nu/2}}\int\prod_{i=1}^{\nu}dy_i\exp\{-[2C(y_1^2+y_2^2+\cdots+y_\nu^2)-2(y_1y_2+y_2y_3+\cdots y_{\nu-1}y_\nu+y_\nu y_1)]\}. \tag{A20}$$

To calculate this integral we consider the bilinear form in the exponent as a scalar product of vectors yA and y, (yA,y), where $y=(y_1,y_2,\ldots,y_\nu)$ and matrix A is

$$A=\begin{pmatrix}2C&-1&0&\cdots&-1\\-1&2C&-1&\cdots&0\\\vdots&\vdots&\vdots&&\\-1&\cdots&\cdots&-1&2C\end{pmatrix}. \tag{A21}$$

Reducing the bilinear form in the exponent (A20) to a quadratic form we rewrite the integral Z_ν as

$$Z_\nu=\frac{1}{\pi^{\nu/2}}\prod_{i=1}^{\nu}\left(\int_{-\infty}^{\infty}dt_i\exp[-\lambda_i t_i^2]\right)=\frac{1}{\sqrt{\lambda_1\ldots\lambda_\nu}}=(\mathrm{Det}A)^{-1/2}. \tag{A22}$$

Here λ_i are the eigenvalues of the matrix A and their product equals to the determinant of A. It is not difficult to show that $\operatorname{Det} A$ can be expressed as

$$\operatorname{Det} A = 2(C\Delta_{\nu-1} - \Delta_{\nu-2} - 1), \tag{A23}$$

where Δ_ν is the determinant of the three-diagonal matrix

$$\begin{pmatrix} 2C & -1 & 0 & \cdots & 0 \\ -1 & 2C & -1 & \cdots & 0 \\ \vdots & \vdots & \vdots & & \\ 0 & \cdots & \cdots & -1 & 2C \end{pmatrix}. \tag{A24}$$

For Δ_ν it is easy to obtain a recurrent formula

$$\Delta_\nu = 2C\Delta_{\nu-1} - \Delta_{\nu-2}. \tag{A25}$$

The ratio $\Delta_\nu/\Delta_{\nu-1}$ satisfies the following relation:

$$\frac{\Delta_\nu}{\Delta_{\nu-1}} = \frac{\sinh(\nu+1)\beta}{\sinh \nu\beta}. \tag{A26}$$

This can be readily verified for $\nu=2,3$, etc. Its proof requires induction to be applied. Consider that this is true for ν. Then it should be valid also for $\nu+1$. We start with Eq. (A25) for $\nu+1$ and use Eq. (A26)

$$\frac{\Delta_{\nu+1}}{\Delta_\nu} = 2C - \frac{\Delta_{\nu-1}}{\Delta_\nu} = \exp\beta + \exp(-\beta) - \frac{\exp\nu\beta - \exp(-\nu\beta)}{\exp(\nu+1)\beta - \exp[-(\nu+1)\beta]} = \frac{\sinh(\nu+2)\beta}{\sinh(\nu+1)\beta}. \tag{A27}$$

So Eq. (A26) is valid. Now as far as

$$\Delta_\nu = \frac{\Delta_\nu}{\Delta_{\nu-1}} \frac{\Delta_{\nu-1}}{\Delta_{\nu-2}} \cdots \frac{\Delta_2}{\Delta_1} \frac{\Delta_1}{\Delta_0}, \quad (\Delta_0 = 1),$$

we apply Eq. (A26) and obtain for Δ_ν

$$\Delta_\nu = \frac{\sinh(\nu+1)\beta}{\sinh\beta}. \tag{A28}$$

Substituting Eqs. (A28) into (A23) we can write for $\operatorname{Det} A$

$$\operatorname{Det} A = 2\left(\cosh\beta \frac{\sinh\nu\beta}{\sinh\beta} - \frac{\sinh(\nu-1)\beta}{\sinh\beta} - 1\right) = \frac{2[\cosh\beta \sinh\nu\beta - (\sinh\nu\beta \cosh\beta - \cosh\nu\beta \sinh\beta) - \sinh\beta]}{\sinh\beta}$$
$$= 2(\cosh\nu\beta - 1) = 4\sinh^2(\nu\beta/2). \tag{A29}$$

So finally we have

$$Z_\nu = \frac{1}{2\sinh(\nu\beta/2)}. \tag{A30}$$

In the d-dimensional case for Z_ν we get Eq. (A30) to the power of d.

Expression (A30) for Z_ν was obtained based on the initial partition function (A9) in the pure Fourier form. It should be pointed out that if we started with the bead-Fourier form with $n>1$ it would result simply in substitution in Eq. (A30) ν by νn and β by β/n which naturally yields the same final formula (A30).

[1] D. M. Ceperley, in *Simulations in Condensed Matter Physics and Chemistry*, edited by K. Binder and G. Cicotti (Editrice Compositori, Bologna, Italy, 1996).

[2] A. P. Lyubartsev and P. N. Vorontsov-Velyaminov, Phys. Rev. A **48**, 4075 (1993).

[3] A. Alavi and D. Frenkel, J. Chem. Phys. **97**, 9249 (1992).

[4] J. S. Hoye and G. Stell, J. Stat. Phys. **77**, 361 (1994).

[5] C. Chakravarty, J. Chem. Phys. **99**, 8038 (1993).

[6] W. H. Newman and A. Kuki, J. Chem. Phys. **96**, 1409 (1992).

[7] R. Q. Topper and D. G. Truhlar, J. Chem. Phys. **97**, 3647 (1992).

[8] G. J. Hogerson and W. P. Reinhardt, J. Chem. Phys. **102**, 4151 (1995).

[9] R. P. Feinman and A. R. Hibbs, *Quantum Mechanics and Path Integrals* (McGraw-Hill, New York, 1965).

[10] W. H. Miller, J. Chem. Phys. **63**, 1166 (1975).

[11] J. D. Doll and D. L. Freeman, J. Chem. Phys. **80**, 2239 (1984); **80**, 5709 (1984).

[12] R. Q. Topper, Q. Zhang, Y.-P. Liu, and D. G. Truhlar, J. Chem. Phys. **98**, 4991 (1993).

[13] R. P. Feinman, *Statistical Mechanics* (Benjamin, New York, 1972).

[14] M. F. Herman, E. J. Bruskin, and B. J. Berne, J. Chem. Phys. **76**, 5150 (1982).

[15] M. Takahashi and M. Imada, J. Phys. Soc. Jpn. **53**, 963 (1984).

[16] P. Elliot and P. G. Dawber, *Symmetry in Physics* (McMillan, London, 1979).

[17] V. Heine and I. A. Abarenkov, Philos. Mag. **9**, 451 (1968).

[18] A. Monnier, V. Srdanov, G. Stucky, and H. Metiu, J. Chem. Phys. **100**, 6944 (1994).

[19] I. S. Gradshteyn and I. M. Ryzhik, *Tables of Integrals, Sums, Series and Products* (Academic, New York, 1965).